Bmp8a Is a Novel Player in Regulation of Antiviral Immunity

Shenjie Zhong[1,2], Haoyi Li[1,2], Yun-Sheng Wang[1,2], Ying Wang[1,2], Guangdong Ji[1,2], Hong-Yan Li[1,2], Shicui Zhang[1,2*], Zhenhui Liu[1,2**]

[1]College of Marine Life Science and Institute of Evolution & Marine Biodiversity, Ocean University of China, Qingdao 266003, China

[2]Laboratory for Marine Biology and Biotechnology, Pilot National Laboratory for Marine Science and Technology (Qingdao), Qingdao 266003, China

*Correspondence author: e-mail: sczhang@ouc.edu.cn

**Correspondence author: e-mail: zhenhuiliu@ouc.edu.cn

Abstract

Bone morphogenetic protein (BMP) is a kind of classical multi-functional growth factor that plays a vital role in the formation and maintenance of bone, cartilage, muscle, blood vessels, and the regulation of energy balance. However, whether BMP plays a role in antiviral immunity is unknown. Here we demonstrate that Bmp8a is a newly-identified positive regulator for antiviral immune responses. The *bmp8a*$^{-/-}$ zebrafish, when infected with the viruses of GCRV, SVCV or TSVDV, show significantly reduced antiviral immunity, increased viral load and morbidity. We also show for the first time that Bmp8a interacts with Alk6a, which promotes the phosphorylation of Tbk1 and Irf3 through p38 MAPK pathway, and induces the production of type I IFNs in response to virus infection. Upon virus infection, *bmp8a* expression is activated through the binding of Stat1a/Stat1b to the GAS motifs in *bmp8a* promoter region, enlarging the antiviral innate immune signal. Our study uncovers a previously unrecognized role of Bmp8a in regulation of antiviral immune responses and provides a new target for controlling viral infection.

60 **Introduction**

61 Viruses infect all groups of living things and produce a variety of diseases. Host cell detection of viral infection
62 depends on the recognition of pathogen-associated molecular patterns (PAMPs) from viral proteins or nucleic
63 acids by the pattern recognition receptors (PRRs) such as Toll-like receptors (TLRs), RIG-I-like receptors (RLRs),
64 NOD-like receptors (NLRs) and cytoplasmic DNA or RNA sensors (***Thaiss et al., 2016; Akira et al., 2003; Chen***
65 ***et al., 2017; Keating et al., 2011; Parvatiyar et al., 2012***). The PRRs, once stimulated by their appropriate ligands,
66 trigger distinct intracellular signaling pathways that converge on the activation of IFN regulatory factor 3 (IRF3)
67 and/or IFN regulatory factor 7 (IRF7), which then translocate into the nucleus and activate the production of
68 interferons (IFNs) that play important roles in inhibiting virus replication (***Honda et al., 2005; Tamura et al., 2008***).

69 IFNs are classified into type I IFNs that include IFNα and IFNβ; type II IFN which has only a single member
70 IFN-γ; and type III IFNs that consist of IFN-λs (***Li et al., 2014***). All these three types of IFNs trigger intracellular
71 signaling cascades generally via the Janus kinase signal transducer and activator of transcription (JAK-STAT)
72 pathway (***Schindler et al., 2008***). Canonically, type I IFNs initiate the signaling via binding to a heterodimeric
73 receptor complex IFN-α/β receptor (IFNAR), inducing phosphorylation of transcription factors STAT1 and STAT2.
74 The phosphorylated STATs form a trimolecular complex with IRF9, which translocates to the nucleus and binds to
75 IFN-stimulated response elements (ISREs) of IFN-stimulated genes (ISGs), resulting in transcriptional activation
76 of the target ISGs, including those encoding numerous cytokines and antiviral proteins (***Decker et al., 1997; Fu***
77 ***et al., 1990; Levy et al., 1989; Levy et al., 1988; Ren et al., 2016; Shuai et al., 1992***). In contrast, type II IFN
78 binds to its unique receptor, IFN-γ receptor (IFNGR), resulting in the phosphorylation of STAT1 and the formation
79 of STAT1 homodimers that recognize gamma-activated sequences (GASs) present in the promoter regions of
80 IFN-γ-regulated genes (***Li et al., 2014***).

81 Bone morphogenetic proteins (BMPs) are potent growth factors belonging to the transforming growth factor
82 beta (TGFβ) superfamily, which are intercellular signaling molecules with multiple functions in development and
83 differentiation, such as skeletal formation and hematopoiesis, as well as lipid oxidation (***Bragdon et al., 2011; Wu***
84 ***et al., 2016***). However, accumulating data suggests that BMPs also play important roles in the regulation of
85 immune responses (***Huber et al., 2011; Martínez et al., 2011; Phillips et al., 2009; Seeger et al., 2015;***
86 ***Takabayashi et al., 2014***). For example, BMP7 has been shown to drive Langerhans cell differentiation (***Yasmin***
87 ***et al., 2013***). Interestingly, BMP signaling appears to have different responses in T cells: BMP4 and BMP6 were
88 shown to promote T cell proliferation, whereas BMP2 was seen to inhibit T cell proliferation (***Sivertsen et al., 2007;***
89 ***Varas et al., 2009***). In addition, although BMPs were found to promote tumor growth by inhibiting the functions of

90 cytotoxic T lymphocytes (CTLs) and dendritic cells (DCs), they were also shown to inhibit cancer cell proliferation
91 and promote the activity of NK cells that typically display antitumour activity (***Chen et al., 2016***). Therefore, it
92 remains controversial regarding the functions of BMPs in immune responses.

93 In humans and mice, two closely related BMP8 genes, *BMP8A* and *BMP8B*, have been identified (***Zhao et***
94 ***al., 1996***). BMP8B has been found to play roles in the regulation of thermogenesis in mature brown adipose tissue
95 and spermatogenesis in male germ cells, while BMP8A shown to closely correlate with the progression of
96 spermatogenesis (***Walton et al., 2016; Ying et al., 2001***). In contrast, only one *bmp8* gene, *bmp8a*, has been
97 isolated in zebrafish, and shown to be involved in the regulation of lipid metabolism (***Zhong et al., 2018***). To date,
98 whether Bmp8a plays a role in immune responses is completely unknown. The present study was thus performed
99 to answer this question. We demonstrated that Bmp8a was a previously unrecognized regulator functioning in
100 antiviral immune responses of zebrafish *Danio rerio*, providing a new target for control of viral infection.

101 **Results**

102 **Bmp8a inhibited RNA virus replication *in vitro*.**

103 To explore the function of zebrafish Bmp8a in the antiviral immune response, we infected both the wild-type
104 zebrafish liver (ZFL) cells and ZFL cells over-expressing bmp8a as well as the epithelioma papulosum cyprini
105 (EPC) cells and EPC cells over-expressing bmp8a with Grass carp reovirus (GCRV), a dsRNA virus, and then
106 monitored the cytopathic effect（CPE）and the viral titers of the supernatants. In response to GCRV challenge,
107 an apparent CPE was observed in the control cells, while the bmp8a-overexpressing ZFL cells had much less CPE
108 (***Figure 1A***). In accordance with the CPE results, a significant decrease of the viral titers was observed in the
109 supernatants of bmp8a-overexpressing ZFL cells (***Figure 1B***). Similarly, the GCRV-induced CPE and GCRV yields
110 of the supernatants were also markedly reduced in the bmp8a-overexpressing EPC cells (***Figure 1C-D***). These
111 suggested that Bmp8a suppressed the replication of the RNA virus in the cells.

112 **Bmp8a was involved in antiviral responses *in vivo*.**

113 To test the function of Bmp8a in host defense against virus infection *in vivo*, we generated *bmp8a* deficient
114 (*bmp8a*$^{-/-}$) zebrafish using the TALEN approach (***Figure 1 – Figure supplement 1A***), which caused 7 nucleotides
115 deletion in the exon 4 (***Figure 1 – Figure supplement 1B-C***). We challenged both the wild-type and *bmp8a*$^{-/-}$
116 mutant zebrafish by intraperitoneal injection with GCRV. Compared with wild-type zebrafish, the levels of GCRV
117 RNA in the liver, kidney, intestine, and spleen of *bmp8a*$^{-/-}$ zebrafish were considerably increased (***Figure 1E***).
118 Accordingly, *bmp8a*$^{-/-}$ zebrafish exhibited significantly reduced survival rate than wild-type zebrafish upon GCRV
119 infection (***Figure 1F***). When the wild-type and *bmp8a*$^{-/-}$ zebrafish were similarly challenged with spring viremia of

120 carp virus (SVCV), a negative ssRNA virus, the survival rate of *bmp8a*$^{-/-}$ zebrafish was also remarkably lower than
121 that of wild-type zebrafish (***Figure 1G***). Moreover, when the wild-type and *bmp8a*$^{-/-}$ zebrafish were infected with
122 turbot skin verruca disease virus (TSVDV) isolated from skin (***Figure 1 – Figure supplement 2***), mortality occurred
123 in *bmp8a*$^{-/-}$ zebrafish at 108 h postinfection, and all the fish died at 156 h post infection, while none of the wild type
124 zebrafish were dead during the period (***Figure 1H***). These data indicated that *bmp8a*$^{-/-}$ zebrafish were more
125 susceptible to virus infection than wild-type zebrafish, suggesting involvement of Bmp8a in antiviral immune
126 responses *in vivo*.

127 **Bmp8a promoted expression of antiviral genes.**

128 In zebrafish, type I IFNs contained 4 members *ifnφ1*, *ifnφ2*, *ifnφ3*, and *ifnφ4*, among which *ifnφ1* and *ifnφ3* were
129 shown to be involved in the antiviral response. In contrast, in carp, only one type I IFN was identified to fulfill
130 antiviral role in EPC cell (***Robertsen, 2006; Zhang et al., 2007***). To pinpoint the role of Bmp8a in the antiviral
131 immune response, both the wild-type and *bmp8a*$^{-/-}$ zebrafish were injected intraperitoneally with GCRV, and the
132 expression of type I IFN genes and the antiviral protein gene *mx* were detected using quantitative reverse
133 transcription PCR (qRT-PCR). We found that the expression of both *ifnφ1* and *ifnφ3* as well as *mx* was all
134 significantly down-regulated in the liver, kidney, intestine, and spleen of *bmp8a*$^{-/-}$ zebrafish, compared with those
135 of wild-type fish (***Figure 2A-D***). We then over-expressed bmp8a in ZFL cells and found that ZFL cells with over-
136 expressed Bmp8a showed markedly higher expression of *ifnφ1*, *ifnφ3*, and *mx* than that of control cells, infected
137 with or without GCRV (***Figure 2E-H***). In addition, *bmp8a* knockdown caused remarkably decreased expression of
138 *ifnφ1*, *ifnφ3*, and *mx* in ZFL cells (***Figure 2I-L***). Similarly, the expression of *ifn* and *mx* in EPC cells with over-
139 expressed Bmp8a was also remarkably up-regulated than that in control cells (***Figure 2M-P***). Moreover, EPC cells
140 cotransfected with bmp8a expressing plasmid and IFNφ1, IFNφ3, or EPC IFN promoter-driven luciferase plasmid,
141 followed by infection with or without GCRV, had markedly increased intracellular IFNφ1, IFNφ3, or EPC IFN
142 promoter-driven luciferase activities (***Figure 2Q-S***). All these data denoted that Bmp8a promoted the expression
143 of both type I IFN and *mx* genes.

144 **Bmp8a activated Tbk1-Irf3-Ifn antiviral signaling via p38 MAPK pathway.**

145 To putatively examine the molecular mechanism by which Bmp8a stimulates *ifn* and *mx* expression, we carried
146 out transcriptome analysis of the livers of *bmp8a*$^{-/-}$ mutant and wild-type zebrafish, that both had been
147 intraperitoneally injected with GCRV. Kyoto Encyclopedia of Genes and Genomes (KEGG) analyses revealed that,
148 compared with wild-type zebrafish, the down-regulated genes in the mutant were remarkably enriched in the RIG-
149 I-like receptor signaling pathway, NF-kappa B signaling pathway, TNF signaling pathway, and protein digestion

150 and absorption that function in the antiviral immune process (***Figure 3 – Figure supplement 1***). In agreement
151 with transcriptome analysis, we found that the expressions of *tbk1*, *irf3*, and *irf7* were significantly upregulated in
152 bmp8a-overexpressing ZFL cells than control cells, infected with or without GCRV (***Figure 3A-D***). Similar
153 expression patterns of *tbk1*, *irf3*, and *irf7* were also observed in EPC cells, infected with or without GCRV (***Figure***
154 ***3E-H***). In addition, *bmp8a* knockdown resulted in considerably reduced expression of *tbk1*, *irf3*, and *irf7* in ZFL
155 cells than control cells, infected with or without GCRV (***Figure 3I-L***). We then evaluated the activation of Tbk1 and
156 Irf3 by immunoblot assays in both bmp8a-overexpressing and wild-type ZFL cells as well as EPC cells, infected
157 with or without GCRV. It was found that phosphorylation levels of Tbk1 and Irf3 were significantly increased in both
158 types of the cells with overexpressed Bmp8a (***Figure 3M-P***). Moreover, *bmp8a* knockdown markedly reduced the
159 phosphorylation levels of Tbk1 and Irf3 in ZFL cells, infected with or without GCRV (***Figure 3Q-R***). Furthermore,
160 in luciferase activity assays, transfection of dominant negative mutations of *tbk1* (tbk1-K38M), *irf3* (irf3DN), or *irf7*
161 (irf7DN) in EPC cells induced a significant loss in the ability of Bmp8a to activate the IFN promoter (***Figure 3S-U***).
162 This was further supported by the observations *in vivo* that the expression of *tbk1*, *irf3*, and *irf7* in the liver, kidney,
163 intestine, and spleen was significantly downregulated in *bmp8a*$^{-/-}$ mutant than that in wild-type zebrafish (***Figure***
164 ***3V-Y***). These data together revealed that Bmp8a induced *ifn* and *mx* expression via promoting Tbk1-Irf3-Ifn
165 antiviral signaling.

166 BMPs transmit signals through smad1/5/8, smad2/3, ERK, JNK, or p38 MAPK pathways (***Derynck et al.,***
167 ***2001; Drummond, 2005; Oh et al.,2002***). Thus, the effects of p38 MAPK inhibitor SB203580, JNK inhibitor
168 SP600125, MEK1/2 inhibitor U0126, SMAD1/5/8 inhibitor DMH1, and smad2/3 inhibitor TP0427736 HCl on the
169 expression of *ifn* was tested in bmp8a-overexpressing ZFL cells and EPC cells. We have shown above that Bmp8a
170 overexpression increased the expression of *ifn* (***Figure 2***). Here we found that only p38 MAPK inhibitor SB203580
171 significantly reduced the expression of *ifnφ1* and *ifnφ3* in ZFL cells and the expression of *ifn* in EPC cells (***Figure***
172 ***4A-C***). Furthermore, the IFN promoter-driven luciferase assays revealed that the luciferase activities were
173 markedly reduced in EPC cells upon treatment with p38 MAPK inhibitor SB203580 (***Figure 4D-F***), consistent with
174 the observation that Bmp8a induced the expression of *ifn* through p38 MAPK pathway. Taken the previous report
175 that the MAPK signaling increased the phosphorylation of TBK1 and IRF3 upon viral infection into consideration
176 (***Shi et al., 2019***), we suggested that Bmp8a activated Tbk1-Irf3-Ifn antiviral signaling via p38 MAPK pathway.

177 **BMP type I receptor Alk6a interacted with Bmp8a and participated in antiviral immunity.**

178 BMPs exert their biological effects through the sequential activation of two types of transmembrane receptors,
179 namely BMP receptor type I and BMP receptor type II, that both possess intrinsic serine/threonine kinase activity

180 (***Heldin et al., 1997; Shi et al., 2003***). To detect which receptor is involved in the regulation of the antiviral immune
181 responses, the expression of both type I receptor genes (*alk2*, *alk3*, *alk6a*) and type II receptor genes (*bmpr2a*,
182 *bmpr2b*, *actr2a*, *actr2b*) in ZFL cells transfected with poly(I:C) or infected with GCRV were measured. Among these
183 receptor genes, *alk6a* showed the highest expression upon poly(I:C) or virus challenge (***Figure 5A-B***). We also
184 overexpressed all these receptors in ZFL and EPC cells, and examined the expression of *ifn* in these cells. The
185 upregulation of *ifnφ1* was only found in the alk6a-overexpressing ZFL cells (***Figure 5C***). Moreover, the
186 overexpression of *alk6a* or *alk2* resulted in significantly increased expression of *ifnφ3* in ZFL cells and *ifn* in EPC
187 cells, with overexpressed *alk6a* being more effective (***Figure 5D-E***). Based on these findings, the function of Alk6a
188 was selected for further test. Compared to wild-type ZFL cells, the expressions of antiviral protein genes *ifnφ1,*
189 *ifnφ3* and *mx* as well as the antiviral signaling genes *tbk1*, *irf3*, and *irf7* were all markedly upregulated in alk6a-
190 overexpressed ZFL cells with or without GCRV infection (***Figure 5F-G***). The similar results were also observed in
191 the alk6a-overexpressed EPC cells (***Figure 5H-I***). Because the phosphorylation of Gly-Ser (GS) domain of the
192 type I receptor is required for its activation, we thus constructed dominant-negative mutant of alk6a (alk6a-ΔGS)
193 plasmid (***Figure 5J***), and then transferred it into both ZFL and EPC cells. It revealed that the dominant-negative
194 mutation of *alk6a* significantly reduced the expression of *mx, ifn* (*ifnφ1* and *ifnφ3* in ZFL cells), *tbk1*, *irf3*, and *irf7*
195 in ZFL and EPC cells, with or without GCRV infection (***Figure 5K-N***). The data suggested that Alk6a was apparently
196 involved in the Tbk1-Irf3/7-Ifn antiviral signaling.

197 Considering we have revealed that Bmp8a activated Tbk1-Irf3-Ifn antiviral signaling via p38 MAPK pathway,
198 we then examined whether the the levels of phosphorylated p38 MAPK protein were regulated by Alk6a. Clearly,
199 compared to wild-type ZFL or EPC cells, phosphorylation levels of p38 MAPK were significantly increased in alk6a-
200 overexpressed both types of the cells with or without GCRV infection (***Figure 6A-D***). Moreover, dominant-negative
201 mutation of *alk6a* significantly reduced the phosphorylation levels of p38 MAPK in ZFL or EPC cells, with or without
202 GCRV infection (***Figure 6E-H***). Thus, Alk6a was shown to be involved in the phosphorylation of p38 MAPK. Next,
203 we investigated whether the antiviral immune responses of Bmp8a were mediated by Alk6a. In the IFN promoter-
204 driven luciferase assays, it was found that the ability of Bmp8a to activate the IFN promoter was markedly blocked
205 after the dominant-negative mutation of *alk6a* in EPC cells (***Figure 6I-K***). Importantly, co-immunoprecipitation (Co-
206 IP) experiments confirmed that Bmp8a interacted with Alk6a (***Figure 6L***). Collectively, our data demonstrated that
207 BMP type I receptor Alk6a interacted with Bmp8a, and participated in the antiviral immunity. To our best knowledge,
208 Alk6a is the first BMP receptor identified thus far which is being directly required for antiviral immune responses.
209

210 **Virus induced expression of *bmp8a*.**

211 Next, we measured the expression of *bmp8a* in ZFL cells upon virus infection. GCRV significantly induced the
212 expression of *bmp8a* at 12 h post-stimulation, and reached a peak at 48 h (***Figure 7A***). We also detected the
213 expression of *bmp8a* upon infection with GCRV or poly(I:C) *in vivo*. The expression of *bmp8a* in the liver, kidney,
214 intestine, and spleen of zebrafish infected with GCRV or poly(I:C) was all significantly elevated (***Figure 7B-I***). This
215 indicated that the expression of *bmp8a* was inducible by infection with virus or its mimic poly(I:C).

216 **Binding of Stat1 to GAS motifs activated *bmp8a* expression.**

217 To explore how virus induces expression of *bmp8a*, we searched for the transcription factor binding sites in *bmp8a*
218 promoter region at the web http://jaspar.genereg.net/. Two gamma-activated sites (GAS), 5'-ATTCCGGGAAA-3'
219 (P1) and 5'-TTTACTAGAAC-3' (P2), in *bmp8a* promoter region were identified (***Figure 8 – Figure supplement 1***).
220 In mammals, the transcription factor STAT1 homodimer was known to bind to the GAS motif in the promoter region
221 of IFN-γ triggered downstream genes (***Decker et al., 1997; Shuai et al., 1992***). We thus wonder if Stat1 can bind
222 to the *bmp8a* promoter region to activate the expression of *bmp8a*. In zebrafish, there exist two Stat1 factors,
223 Stat1a (GenBank accession number NM_131480.1) and Stat1b (GenBank accession number NM_200091.2).
224 Thus we constructed dominant-negative mutant plasmids of stat1a-ΔC and stat1b-ΔC, that were transferred into
225 ZFL cells, respectively. It was found that the expression of *bmp8a* was significantly blocked in both cases (***Figure***
226 ***8A-B***). By contrast, the overexpression of either *stat1a* or *stat1b* markedly promoted *bmp8a* promoter-driven
227 luciferase activities (***Figure 8C***). In addition, when one of the GAS motifs in *bmp8a* promoter region was deleted,
228 *bmp8a* promoter-driven luciferase activities were significantly reduced; when both of the GAS motifs were deleted,
229 *bmp8a* promoter-driven luciferase activities were reduced even more significantly (***Figure 8D-E***). These suggested
230 that both Stat1a and Stat1b may interact with the GAS motifs.

231 To verity the binding of Stat1a/Stat1b to the GAS motifs in *bmp8a* promoter region, the recombinant proteins
232 of both Stat1a and Stat1b were expressed and purified (***Figure 8F-G***), and used for electrophoretic mobility shift
233 assay (EMSA). As shown in ***Figure 8H-K***, a remarkable band of protein-DNA complex was observed (lane 2). The
234 protein-DNA complex band was obviously weaker in the presence of an excess unlabeled competitor probe,
235 compared to that of biotin labeled probe group (lane 3), but the intensity of the band showed little change in the
236 presence of GAS mutant probes (lane 4). To detect the specific binding, a supershift experiment with the antibody
237 against His tag was performed. It revealed that His tag antibody caused a specific supershift of slower migrating
238 protein-DNA-antibody complex (***Figure 8H-K***, lane 5). There was no protein-DNA complex observed in the
239 negative control group (***Figure 8H-K***, lane 1). These demonstrated that both Stat1a and Stat1b could directly bind

240 to the GAS motifs in *bmp8a* promoter region, suggesting that *bmp8a* expression was subjected to the regulation
241 by binding of Stat1a/Stat1b to the GAS motifs.

242 **Discussion**

243 BMPs, canonical multi-functional growth factors, are suggested to play roles in regulation of immune
244 responses, but it remains controversial over their functions in immunity. We show here for the first time that Bmp8a
245 is a previously unrecognized factor involved in the regulation of antiviral immune responses in zebrafish. Evidences
246 supporting this nature of Bmp8a include: Bmp8a inhibits RNA viruses replication *in vitro* and *in vivo*; Bmp8a promotes
247 the expression of antiviral protein genes including type I IFNs and *mx*; the expression of *bmp8a* is induced by CGRV
248 or poly(I:C), and Bmp8a activates TBK1-IRF3-IFN signaling. Bmp8a is a member of the TGF-β superfamily, which
249 includes more than 30 genes encoding TGFβ, BMPs and activins. TGFβ has been shown to have both pro- and
250 anti-inflammatory effects depending on the context it is acting in the immune system (***Worthington et al., 2012***).
251 Like TGFβ, BMP members have also been shown to play different immunoregulatory roles (***Tu et al., 2014***). BMP2,
252 4 and 7 deficiency or knockdown results in partial loss of the thymic capsule, reduced size of thymus and increased
253 *Helicobacter pylori*-induced inflammation, whereas BMP6 inhibits macrophage growth by inducing cell cycle arrest
254 *in vitro* (***Aleman-Muench and Soldevila, 2012; Takabayashi et al., 2014; Bleul et al., 2005; Gordon et al., 2010;***
255 ***Lee et al., 2007***). The finding that Bmp8a is a positive regulator in antiviral immune responses provides a new
256 angle for our understanding of the functions of TGF-β superfamily members including BMPs.

257 On one hand, it is generally regarded that the recognition of virus by PRRs elicits the activation of IRF3 and
258 NF-κB, and induces the production of IFNα/β, that then activate JAK-STAT pathway, eventually leading to the
259 production of ISGs such as cytokines and antiviral proteins. On the other hand, BMPs are known to transmit signals
260 through both Smad-dependent pathways (smad1/5/8 and smad2/3 pathways) and Smad-independent pathways
261 (ERK, JNK, and p38 MAPK pathways). Here we clearly demonstrate that Bmp8a promotes the expression of
262 endogenous type I IFNs independent of Smad signaling pathways. Moreover, it is p38 MAPK pathway, rather than
263 ERK and JNK pathways, that is involved in the antiviral responses induced by Bmp8a. Furthermore, we show that
264 Alk6a participates in Tbk1-Irf3/7-Ifn antiviral signaling via interaction with Bmp8a. In addition, Alk6a was found to
265 be required to induce the phosphorylation of p38 MAPK, which is consistent with the findings in mouse that Alk6
266 knockdown suppresses p38 MAPK phosphorylation (***Itoh et al., 2008***). Previous studies have shown that MAPK
267 signaling pathway is crucial in the phosphorylation of TBK1 and IRF3 upon viral infection (***Shi et al., 2019***). Thus,
268 we probably discover a new pathway of Bmp8a signaling in antiviral immune responses that Bmp8a acts as a
269 positive regulator through the promotion of phosphorylation of Tbk1 via p38 MAPK pathway, i.e., Bmp8a binds to

270 Alk6a, which induces p38 MAPK phosphorylation, and in turn enhances Tbk1 and Irf3 phosphorylation, eventually
271 resulting in increased synthesis of type I IFN (***Figure 9***).

272 Our study also show that the challenge with GCRV and poly(I:C) both significantly promotes the expression
273 of zebrafish *bmp8a*. Searching for the binding sites of transcript factors in *bmp8a* promoter region reveals that two
274 IFN-γ activation sites (GAS) that may interact with STAT1 are identified. Functionally, we demonstrate that Stat1a
275 and Stat1b, orthologues of human STAT1, can directly bind the GAS sites in *bmp8a* promoter, resulting in activation
276 of *bmp8a* expression. It has been reported that in black carp, Stat1a and Stat1b can both form homodimer and
277 heterodimer *in vivo* like their mammalian counterpart (***Wu et al., 2019***). It is thus highly likely that in zebrafish,
278 Stat1a and Stat1b can form homodimer or heterodimer, which then binds to the GAS sites in *bmp8a* promoter
279 region. In zebrafish, IFN-γ has been found to be able to induce the expression of both *stat1a* and *stat1b*, and the
280 GAS motif is required for Ifn-γ activation (***Zou and Secombes, 2011; Ruan et al., 2017***). It is widely known that
281 the JAK-STAT pathway is one of the most important candidate pathways through which IFN-γ works. Activation of
282 JAK-STAT signaling leads to transcription of various downstream ISGs for antiviral activity (***Boehm et al., 1997***).
283 We thus think that Bmp8a is another important antiviral factor which can be activated through Ifn-γ-Jak-Stat1
284 pathway (***Figure 9***).

285 In summary, we demonstrate for the first time that Bmp8a is a positive regulator in antiviral immune responses,
286 which functions through promotion of phosphorylation of Tbk1 via p38 MAPK pathway. Upon virus infection, the
287 expression of *bmp8a* is activated by Stat1a/Stat1b directly. Bmp8a knockdown leads to significantly decreased
288 phosphorylation of Tbk1 and Irf3. As a consequence, *bmp8a*-deficient zebrafish produces significantly lowered
289 type I IFNs in response to RNA virus infection, exhibits significantly reduced immune responses, and increases
290 significantly higher viral load and morbidity *in vivo*. Our study is significant to understand the regulatory mechanism
291 of BMP involving in antiviral immune response and provides a new target for controlling viral infection.
292
293
294
295
296
297
298
299

300 **Materials and Methods**

301 **Key Resources Table**

Reagent type (species) or resource	Designation	Source or reference	Identifiers	Additional information
antibody	anti-TBK1 (rabbit, monoclonal)	Cell Signaling Technology	3504	WB(1:1000)
antibody	anti-TBK1 pSer172 (rabbit, monoclonal)	Cell Signaling Technology	5483	WB(1:1000)
antibody	anti-IRF3 (rabbit, polyclonal)	Bioss	2993R	WB(1:1000)
antibody	anti-IRF3 pSer386 (rabbit, monoclonal)	Bioss	52170R	WB(1:1000)
antibody	anti-p38MAPK (rabbit, polyclonal)	Bioss	0637R	WB(1:1000)
antibody	anti-p38 MAPK pThr180/pTyr182 (rabbit, polyclonal)	Bioss	2210R	WB(1:1000)
antibody	anti-β-Actin (rabbit, polyclonal)	Bioss	0061R	WB(1:2000)
antibody	anti-HA (mouse, monoclonal)	Beyotime	AH158	WB(1:1000)
antibody	anti-Falg (mouse, monoclonal)	Beyotime	AF519	WB(1:1000)
antibody	anti-His (mouse, monoclonal)	CWBIO	CW0285	WB(1:5000)
antibody	goat anti-rabbit IgG HRP	CWBIO	CW0103S	WB(1:8000)
antibody	VeriBlot for IP Detection	Abcam	ab131366	WB(1:5000)
other	Protein A/G PLUS-Agarose	Santa Cruz	sc-2003	
kit	Chemiluminescent EMSA Kit	Beyotime	GS009	
kit	PrimeScript™ RT reagent Kit with gDNA Eraser	TaKaRa	RP047A	
kit	miRNeasy Mini Kit	QIAGEN	217004	
chemical compound	DMH1	Selleck	S7146	10 μM
chemical compound	TP0427736 HCl	Selleck	S8700	10 μM
chemical compound	SB203580	Beyotime	S1863	10 μM
chemical compound	SP600125	Beyotime	S1876	10 μM
chemical compound	U0126	Beyotime	S1901	10 μM
kit	Lipofectamine RNAiMAX	Invitrogen	13778075	
kit	Luc-Pair Duo-Luciferase Assay Kits	iGene Biotechnology	LF002	
kit	FuGENE HD Transfection Reagent	Promega	E2311	
kit	Mut Express II Fast Mutagenesis Kit	Vazyme	C214-01	
kit	mMESSAGE mMACHINE SP6 kit	Invitrogen	AM1340	

302 **Cells and viruses.** The epithelioma papulosum cyprini cells (EPC), zebrafish liver cells (ZFL) were acquired from

303 the China Zebrafish Resource Center (CZRC) and cultured according to the instructions from the CZRC. EPC and

304 ZFL cells were grown in a 28 °C incubator supplied with 5% CO_2. The flounder gill cells (FG) were grown in a 22 °C

305 incubator supplied. The EPC or FG cells were cultured in MEM media supplemented with 10% fetal bovine serum

306 (FBS), 100 U/ml penicillin and 100 μg/ml streptomycin. The ZFL cells were maintained in DMEM/F-12 media
307 supplemented with 10% FBS, 100 U/ml penicillin and 100 μg/ml streptomycin. Grass carp reovirus (GCRV), a
308 dsRNA virus, and spring viremia of carp virus (SVCV), a negative ssRNA virus, were kindly provided by Yibing
309 Zhang (Institute of Hydrobiology, Chinese Academy of Sciences), and tittered according to the method of Reed
310 and Muench (***Reed and Muench, 1938***), by a 50% tissue culture infective dose ($TCID_{50}$) assay on EPC cells. The
311 turbot skin verruca disease virus (TSVDV) was isolated from the focal site of turbot skin in our lab.

312 **Zebrafish**. The zebrafish *bmp8a* knockout mutant lines (*bmp8a*$^{-/-}$) were established from the zebrafish AB line
313 using TALENs technology. The TALENs for zebrafish *bmp8a* were assembled using the Unit Assembly (UA)
314 method as previously described (***Huang et al., 2014***). All the UA method starting vectors were the gifts from
315 laboratories of Bo Zhang at Peking University and of Shuo Lin at University of California Los Angeles. TALENs
316 mRNAs were transcribed using the mMESSAGE mMACHINE SP6 kit and purifified using the RNeasy Mini kit. To
317 generate zebrafish mutant lines, TALEN mRNAs (50–200 pg) were microinjected into 1-cell stage zebrafish
318 embryos. Two days after injection, genomic DNA was isolated from 8 to 10 pooled larvae. The target genomic
319 regions were amplified by nested PCR and subcloned into the pGEM-T vector. Single colonies were genotyped by
320 sequencing. To obtain germline mutations, the TALEN-injected embryos were raised to adulthood and outcrossed
321 with wild-type (WT) fish. The F1 progeny were genotyped by sequencing. To obtain homozygous mutants,
322 heterozygous mutant of the same mutation were obtained and self-crossed. The primers used in this study were
323 listed in Supplemental Table 1.

324 **Plasmid construction.** The open reading frames (ORF) of zebrafish bmp8a, stat1a, stat1b, alk2, alk3, alk6a,
325 actr2a, actr2b, bmpr2a and bmpr2b were cloned into the pcDNA3.1 expression vector for the eukaryotic expression.
326 The ORF of zebrafish stat1a and stat1b were cloned into the pET-28a expression vector for the expression of
327 recombinant proteins. The promoter regions of bmp8a, bmp8a-ΔP1 (delete the GAS motif of 5´-attccgggaaa-3´ in
328 the bmp8a promoter), bmp8a-ΔP2 (delete another GAS motif of 5´-tttactagaac-3´ in the bmp8a promoter), bmp8a-
329 ΔP1and ΔP2 (delete both the two GAS motifs), IFNφ1, IFNφ3, and EPC IFN were cloned into the pGL3-basic
330 vector. Dominant negative mutant plasmids including tbk1-K38M, stat1a-ΔC, stat1b-ΔC, irf3DN, and irf7DN were
331 described previously (***Feng et al., 2015; Sun et al., 2011***). Dominant negative mutant plasmids alk6a-ΔGS (delete
332 the sequence of 5´-agctccggttctggctcagga-3´ encoding the GS domain) was cloned into the pcDNA3.1 expression
333 vector. The deletions and mutations were created using Mut Express II Fast Mutagenesis Kit. The primers used in
334 this study were listed in Supplemental Table 2.

335 **Transcriptome Sequencing.** The zebrafish were fasted for 24 h prior to tissue collection. Three mutant (*bmp8a*-

336 $^{/-}$) and three wild type (WT) adult zebrafish (0.4 g ± 0.05 g) were randomly selected from each group and were
337 injected intraperitoneally with 50 μl of GCRV (10^8TCID$_{50}$ per ml) per fish. Seventy-two hours after the injection, the
338 livers from three fish each group were pooled together for total RNA extraction. Three independent samples from
339 each group were prepared for transcriptome sequencing. mRNAs were enriched by magnetic beads combining
340 the oligo (dT). cDNA fragments were subjected to the end repair process by the addition of a single 'A' base and
341 the ligation of Illumina sequencing adapters. The ligation products were selected by agarose gel electrophoresis,
342 amplified by PCR, and sequenced using Illumina HiSeq 4000 by Annoroad Technology (Beijing, China).
343 **Identification of DEGs.** The RPKM (reads per kb per million reads) method was used to calculate and normalize
344 the abundances of genes (***Mortazavi et al., 2008***). DEGs across groups were identified by the edgeR package
345 (http://www.r-project.org/). Genes with a fold change ≥ 2 and a false discovery rate (FDR) < 0.05 in a comparison
346 were regarded as significantly expressed. DEGs were then subjected to enrichment analysis of KEGG pathways.
347 **Viral infection *in vitro***. EPC, FG, or ZFL cells were plated 24 h before infection. Cells were infected with GCRV
348 (5 × 10^4TCID$_{50}$ per ml) or TSVDV (crude virus extracts filtered by a 0.45 μm microporous membrane) for 1 h in
349 medium without FBS. After infection, cells were washed with PBS and then medium was added with FBS. The
350 cells and cell-free supernatants were harvested at the indicated times.
351 **Viral infection *in vivo***. For *in vivo* viral infection, the adult WT and *bmp8a*$^{-/-}$ zebrafish were infected via
352 intraperitoneal injection using 50 μL of SVCV (10^8TCID$_{50}$ per ml), GCRV (10^8TCID$_{50}$ per ml), or TSVDV (crude
353 virus extracts filtered by a 0.45 μm microporous membrane) per fish. Total RNA was extracted and viral RNA
354 expression in the liver, kidney, intestine, and spleen were examined by qRT-PCR. For the survival experiments,
355 zebrafish were monitored for survival after SVCV, GCRV, or TSVDV infection.
356 **Crystal violet staining**. EPC or ZFL cells were transfected with bmp8a or empty vector plasmid. At 24 h post
357 transfection, cells were treated with GCRV (5 × 10^4TCID$_{50}$ per ml). At 72 h after virus challenge, cells were fixed
358 with 4% formaldehyde for 1 h and stained with 0.5% crystal violet for 2 h. After washing with tap water, visible
359 plaques were photographed.
360 **Luciferase assays.** EPC cells were seeded in 24-well plates overnight and cotransfected with various plasmids
361 using FuGENE HD Transfection Reagent following the manufacturer's instruction. If necessary, the cells were
362 infected with GCRV (5 × 10^4TCID$_{50}$ per ml). At the indicated time points, luciferase activities were measured with
363 the Luc-Pair Duo-Luciferase Assay Kits. Data were normalized by calculating the ratio between firefly luciferase
364 activity and *Renilla* luciferase activity. The primers used for cloning the promoter are shown in
365 Supplemental Table 2.

366 **RNA interference.** Small interfering RNA (siRNA) of bmp8a and si-NC (negative control) were purchased from
367 RiboBio. The oligonucleotide sequences (siRNA) specific targeting *bmp8a* mRNA was as follows: 5´-
368 GTTCTTCAGAGCTAGTCAA-3´. Transfection was performed with Lipofectamine RNAiMAX according to the
369 manufacturer's protocols. Total RNA was extracted for qRT-PCR analysis.

370 **Drug treatment and analysis.** SMAD1/5/8 inhibitor DMH1, smad2/3 inhibitor TP0427736 HCl, p38 MAPK inhibitor
371 SB203580, JNK inhibitor SP600125, and MEK1/2 inhibitor U0126 were dissolved in dimethyl ulfoxide (DMSO).
372 ZFL or EPC cells were treated with each inhibitor, which were diluted with culture medium at concentrations of 10
373 μM for 24 h. Total cellular RNA was extracted for qRT-PCR analysis.

374 **RNA quantification.** Total RNA was isolated using the miRNeasy Mini Kit according to the manufacturer's
375 instructions. RNA treated with DNase and the cDNAs were synthesized with PrimeScript™ RT reagent Kit with
376 gDNA Eraser. Samples without reverse transcriptase were also added as control. Gene expression was
377 determined by amplifying the cDNA with ChamQ SYBR Color qPCR Master Mix by an ABI 7500 Fast Real-Time
378 PCR System. The expression of zebrafish *actb1* or EPC *actin* was used as an internal control. The $2^{-\Delta\Delta Ct}$ method
379 was used to calculate relative expression changes. All qRT-PCR experiments were performed in triplicate and
380 repeated three times. Primers used are listed in Supplementary Table 1.

381 **Preparation of recombinant protein.** The recombinant protein of rStat1a or rStat1b was expressed and purified
382 as previous description (***Sun et al., 2013***). Briefly, the recombinant plasmid (pET-28a-stat1a or pET-28a-stat1b)
383 was transformed into *Trans*B (DE3) chemically competent cell. The positive transformants were incubated in liquid
384 LB medium containing 50 μg/mL kanamycin at 37 °C by shaking at 160 rpm. When the cells grow to OD600 = 0.5,
385 isopropyl β-D-thiogalactoside (IPTG) was added to a final concentration of 1 mM, and incubated at 19 °C with
386 shaking at 120 rpm for 14 h. After incubation, the cells were harvested by centrifugation, re-suspended in PBS,
387 and broken by ultrasound. The supernatant was centrifuged at 12,000 g for 20 min, and the protein was purified
388 by Ni-NTA Sepharose column. The concentration of purified protein was determined by BCA (bicinchonininc acid)
389 method. The purified recombinant proteins were stored at -80 °C for subsequent experiment.

390 **Electrophoretic mobility shift assay.** Electrophoretic mobility shift assay (EMSA) was performed according to
391 the instruction of Chemiluminescent EMSA Kit. Oligonucleotides (Supplementary Table 1) were synthesized and
392 biotinylated by Sangon Biotech Company as required and the complementary oligonucleotides were annealed to
393 form the double DNA probe. The recombinant protein was pre-incubated in EMSA/Gel-Shift binding buffer with
394 poly (dI-dC) at 25 °C for 25 min in the presence or absence of Non-Biotin probe (0.5 μM). Then, all samples were
395 mixed with biotinylated probes (0.5 μM) and incubated at 25°C for 30 min. The binding reaction without

396 recombinant protein was set as the negative control. For supershift analysis, anti-His tag antibody was incubated
397 with the reaction mixture for another 30 min after the labeled probe was added. After separation in a native 6%
398 polyacrylamide gel, the free probes and DNA-protein compound were transferred to a Hybond-N^+ nylon membrane,
399 followed by crosslinking under UV light. After immersion in the blocking buffer, membranes were incubated with
400 streptavidin conjugated HRP for 20 min with shaking and then washed three times with washing buffer. Membranes
401 were exposed briefly in Western Lightning-ECL and then exposure to Automatic X-ray Film Processor.

402 **Immunoblot analysis and co-immunoprecipitation.** For Immunoblot analysis, cells were lysed in NP-40 buffer
403 (150 mM NaCl, 0.5% EDTA, 50 mM Tris, 1% NP40, proteinase inhibitors, and protein phosphatase inhibitors) for
404 30 min on ice. For co-immunoprecipitation (co-IP), whole-cell extracts were collected 48 h after transfection and
405 lysed in NP-40 buffer on ice for 30 min. After centrifugation for 15 min at 12,000 × g, 4 °C, supernatants were
406 collected and incubated with Protein A/G PLUS-Agarose coupled to specific antibodies for overnight with rotation
407 at 4°C. Beads were washed 3 × times with NP-40 buffer. Bound proteins were eluted by boiling 7min with 2 x SDS
408 sample buffer. For immunoblot analysis, immunoprecipitates or whole-cell lysates were separated by 12.5% SDS–
409 PAGE gels, electro-transferred to PVDF membranes and blocked for 4 h with 5% no-fat milk solution, followed by
410 blotting with the appropriate antibodies and detection by enhanced chemiluminiscence (ECL). Antibodies from Cell
411 Signaling Technology: anti-TBK1 and anti-TBK1 pSer172. Antibodies from Bioss: anti-IRF3, anti-IRF3 pSer386,
412 anti-p38MAPK, anti-p38 MAPK pThr180/pTyr182, anti-β-Actin. Antibodies from Beyotime: anti-HA and anti-Falg.
413 Antibodies from CWBIO: anti-His and goat anti-rabbit IgG HRP secondary antibody. Antibodies from Abcam:
414 VeriBlot for IP Detection.

415 **Statistical analysis.** Representative experiments have been repeated at least two to three times. All statistical
416 analysis was performed using Graphpad Prism 8.0.1. Data are presented as mean ± SEM. Statistical significance
417 was assessed using the unpaired, two-tailed Student's *t*-test. Survival analyses were performed using the Kaplan-
418 Meier method and assessed using the log-rank (Mantel-Cox) test. *$p < 0.05$, **$p < 0.01$, *** $p < 0.001$; ns, non-
419 significant, $p > 0.05$.

420 **Data availability.** All data are available from the corresponding author upon reasonable request and that a Source
421 Data file is available for this article.

422 **Conflict of Interest**

423 The work is under a patent in China "A method to improve the antiviral immunity of fish (Application No.
424 201910454499.6)".

425 **Author contributions**

426 Z.L.and S.-C.Z. conceived and coordinated the project. Z.L., G.J., and S.Z. designed the experiments. S.Z.,

427 H.L. and Y.-S.W. performed experiments. H.-Y.L. and Y.W. contributed to establish the *bmp8a* knockout mutant
428 lines (*bmp8a*$^{-/-}$) using TALENs technology. S.Z. performed the statistical analysis. Z.L., S.-C.Z. and S.Z. wrote the
429 manuscript, with input from the other authors. All authors reviewed the manuscript and approved the final version.

430 **Acknowledgements**

431 This work was supported by the grants of National Natural Science Foundation of China (31572259) and
432 National Key Research and Development Project of the Ministry of Science and Technology (2018YFD0900505).

433 **Ethics**

434 Animal experimentation: The animals used in the experiment followed the ethical guidelines established by the
435 Institutional Animal Care and Use Committee of the Ocean University of China (permit number, SD2007695).

436
437
438
439
440
441
442
443
444
445
446
447
448
449
450
451
452
453
454
455
456

457 **Figure legends**

458 **Figure 1. Bmp8a inhibits RNA virus replication both *in vitro* and *in vivo*.** (**A**, **B**) ZFL cells were transfected
459 with bmp8a or empty vector, respectively. The cells were infected with GCRV (5 × 10^4TCID$_{50}$ per ml) at 24 h post-
460 transfection, and the culture supernatants were collected at 72 h post-infection. The cell monolayers were fixed
461 with 4% paraformaldehyde for 1 h and stained with 0.5% crystal violet for 2 h (**A**), and the viral titers of the
462 supernatants were determined by TCID$_{50}$ assays (**B**). (**C**, **D**) Similar as (**A**, **B**) but in EPC cells. (**E**) The expression
463 of GCRV RNA in the liver, kidney, intestine, and spleen from wild-type (WT) or *bmp8a*$^{-/-}$ zebrafish injected i.p. with
464 50 μl of GCRV (10^8TCID$_{50}$ per ml) for 72 h. (**B, D, E**) Data were from three independent experiments. Values are
465 expressed as mean ± SEM and analyzed by Student's *t*-test (***p < 0.001). (**F**, **G**) Survival curve of WT and *bmp8a*$^{-}$
466 $^{/-}$ zebrafish i.p. injected with 50 μl of GCRV (10^8TCID$_{50}$ per ml) or SVCV (10^8TCID$_{50}$ per ml). Values are expressed
467 as percent survival of 20 zebrafish for each genotype. *p<0.05 by log-rank test. (**H**) Survival curve of WT and
468 *bmp8a*$^{-/-}$ zebrafish i.p. injectedwith 50 μl of TSVDV (crude virus extracts filtered by a 0.45 μm microporous
469 membrane). Values are expressed as percent survival of 8 zebrafish for each genotype. **p<0.01 by log-rank test.
470 Source data are provided as a Source Data file.

471 **Figure 2. Bmp8a promotes antiviral innate immune responses.** (**A**–**D**) Expression of *ifnφ1*, *ifnφ3*, and *mx*
472 mRNA in the liver (**A**), kidney (**B**), intestine (**C**), and spleen (**D**) from WT or *bmp8a*$^{-/-}$ zebrafish injected i.p. with 50
473 μl of GCRV (10^8TCID$_{50}$ per ml) for 72 h. (**E**, **F**) Expression of *ifnφ1*, *ifnφ3*, and *mx* mRNA after transfected with
474 bmp8a or empty vector in ZFL cells. The cells were collected at 36 h (**E**) or 48 h (**F**) post transfection. (**G**, **H**)
475 Expression of *ifnφ1*, *ifnφ3*, and *mx* mRNA after transfected with bmp8a or empty vector in ZFL cells for 24 h,
476 followed by infection with GCRV (5 × 10^4TCID$_{50}$ per ml) for another 24 h (**G**) or 36 h (**H**). (**I**, **L**) Expression of *ifnφ1*,
477 *ifnφ3*, and *mx* mRNA after *bmp8a* knockdown in ZFL cells. The cells were collected at 36 h (**I**) or 48 h (**L**) post
478 knockdown. (**K**, **L**) Expression of *ifnφ1*, *ifnφ3*, and *mx* mRNA after knockdown *bmp8a* in ZFL cells for 24 h, followed
479 by infection with GCRV (5 × 10^4TCID$_{50}$ per ml) for another 24h (**K**) or 36 h (**L**). (**M**, **N**) Expression of EPC *ifn* and
480 EPC *mx* mRNA after transfected with bmp8a or empty vector in EPC cells. The cells were collected at 36 h (**M**) or
481 48 h (**N**) post transfection. (**O**, **P**) Expression of EPC *ifn* and EPC *mx* mRNA after transfected with bmp8a or empty
482 vector in EPC cells for 24 h, followed by infection with GCRV (5 × 10^4TCID$_{50}$ per ml) for another 24 h (**O**) or 36 h
483 (**P**). (**Q**–**S**) EPC cells were transfected with pGL3-IFNφ1-promoter-luc (**Q**), pGL3-IFNφ3-promoter-luc (**R**) or pGL3-
484 EPC IFN-promoter-luc (**S**) respectively, with or without bmp8a, followed by infection with GCRV (5 × 10^4TCID$_{50}$ per
485 ml). *Renilla* luciferase was used as the internal control. Data were from three independent experiments. Values are
486 expressed as mean ± SEM and analyzed by Student's *t*-test (*p < 0.05, **p < 0.01, ***p < 0.001). Source data are

487 provided as a Source Data file.

488 **Figure 3. Bmp8a increases Tbk1-Irf3-Ifn antiviral signaling.** (**A**, **B**, **E**, **F**) Expression of *irf3*, *irf7*, and *tbk1* mRNA
489 after transfected with bmp8a or empty vector in ZFL (**A**, **B**) or EPC (**E**, **F**) cells. The cells were collected at 36 h
490 (**A**, **E**) or 48 h (**B**, **F**) post transfection. (**C**, **D**, **G**, **H**) Expression of *irf3*, *irf7*, and *tbk1* mRNA after transfected with
491 bmp8a or empty vector in ZFL (**C**, **D**) or EPC (**G**, **H**) cells for 24 h, followed by infection with GCRV ($5 \times 10^4 TCID_{50}$
492 per ml) for another 24 h (**C**, **G**) or 36 h (**D**, **H**). (**I, J, K, L**) Expression of *irf3*, *irf7*, and *tbk1* mRNA after *bmp8a*
493 knockdown in ZFL cells. The cells were collected at 36 h (**I**) and 48 h (**J**) post knockdown or at 24 h (**K**) and 36 h
494 (**L**) post infected with GCRV ($5 \times 10^4 TCID_{50}$ per ml). (**M**, **O**) Immunoblot analysis of phosphorylated (p-) Tbk1 and
495 Irf3 after transfected with bmp8a or empty vector in ZFL (**M**) or EPC (**O**) cells. The cells were collected at 36 h or
496 48 h post transfection for Immunoblot analysis. (**N**, **P**) Immunoblot analysis of phosphorylated (p-) Tbk1 and Irf3
497 after transfected with bmp8a or empty vector in ZFL (**N**) or EPC (**P**) cells for 24 h, followed by infection with GCRV
498 ($5 \times 10^4 TCID_{50}$ per ml) for another 24 h or 36 h. (**Q**, **R**) Immunoblot analysis of phosphorylated (p-) TBK1 and IRF3
499 after *bmp8a* knockdown in ZFL cells. The cells were collected at 36 h and 48 h post knockdown or at 24 h and 36
500 h post infected with GCRV ($5 \times 10^4 TCID_{50}$ per ml). (**S**–**U**) EPC cells were cotransfected with pGL3-IFNφ1-promoter-
501 luc (**S**), pGL3-IFNφ3-promoter-luc (**T**) or pGL3-EPC IFN-promoter-luc (**U**), and bmp8a together with each of the
502 dominant negative plasmids including tbk1-K38M, irf3DN and irf7DN. At 48 h post transfection, the cells were
503 collected for luciferase assays. *Renilla* luciferase was used as the internal control. (**V**–**Y**) Expression of *irf3*, *irf7*,
504 and *tbk1* mRNA in the liver (**V**), kidney (**W**), intestine (**X**), and spleen (**Y**) from WT or *bmp8a*$^{-/-}$ zebrafish injected
505 i.p. with 50 μl of GCRV ($10^8 TCID_{50}$ per ml). Data were from three independent experiments. Values are expressed as
506 mean ± SEM and analyzed by Student's *t*-test (**$p < 0.01$, ***$p < 0.001$). Source data are provided as a Source
507 Data file.

508 **Figure 4. Bmp8a promotes the IFN expression via p38 MAPK pathway.** (**A, B**) Expression of *ifnφ1* (**A**) and
509 *ifnφ3* (**B**) mRNA after transfected with bmp8a in ZFL cells for 24 h, followed by treatment with SB203580,
510 SP600125, U0126, DMH1 and TP0427736 HCl for another 24 h. **C** similar as (**A**, **B**) but in EPC cells. (**D**–**F**) EPC
511 cells were cotransfected with pGL3-IFNφ1-promoter-luc (**D**), pGL3-IFNφ1-promoter-luc (**E**) or pGL3-EPC IFN-
512 promoter-luc (**F**), pRL-TK together with bmp8a or empty vector, respectively. At 24 h post transfection, cells were
513 treated with or without SB203580 for another 24 h and then harvested for detection of luciferase activity. *Renilla*
514 luciferase was used as the internal control. Data were from three independent experiments. Values are expressed
515 as mean ± SEM and analyzed by Student's *t*-test (**$p < 0.01$, ***$p < 0.001$). Source data are provided as a Source
516 Data file.

517 **Figure 5. Alk6a is involved in the antiviral innate immune responses.** (**A, B**) Expression of *alk2*, *alk3*, *alk6a*,
518 *bmpr2a*, *bmpr2b*, *actr2a*, *actr2b* mRNA in ZFL cells stimulated with GCRV (5 × 10^4TCID$_{50}$ per ml, **A**) or poly(I:C)
519 (2 μg/ml, **B**) for 48 h. (**C**–**E**) Expression of *ifnφ1* (**C**) and *ifnφ3* (**D**) mRNA in ZFL cells or EPC *ifn* (**E**) in EPC cells
520 which were transfected with alk2, alk3, alk6a, bmpr2a, bmpr2b, actr2a, actr2b or empty vector for 48 h. (**F, H**)
521 Expression of *irf3*, *irf7*, *tbk1*, *ifn* (or *ifnφ1* and *ifnφ3*), and *mx* mRNA after transfected with alk6a or empty vector in
522 ZFL (**F**) or EPC (**H**) cells for 48 h. (**G, I**) Expression of *irf3*, *irf7*, *tbk1*, *ifn* (or *ifnφ1* and *ifnφ3*), and *mx* mRNA after
523 transfected with alk6a or empty vector in ZFL (**G**) or EPC (**I**) cells for 24 h, followed by infection with GCRV (5 ×
524 10^4TCID$_{50}$ per ml) for another 36 h. **J** Schematic drawing of the alk6a-ΔGS mutation that the GS domain of Alk6a
525 was deleted. (**K**, **M**) Expression of *irf3*, *irf7*, *tbk1*, *ifn* (or *ifnφ1* and *ifnφ3*), and *mx* mRNA after transfected with
526 alk6a-ΔGS or empty vector in ZFL (**K**) or EPC (**M**) cells for 48 h. (**L, N**) Expression of *irf3*, *irf7*, *tbk1*, *ifn* (or *ifnφ1*
527 and *ifnφ3*), and *mx* mRNA after transfected with alk6a-ΔGS or empty vector in ZFL (**L**) or EPC (**N**) cells for 24 h,
528 followed by infection with GCRV (5 × 10^4TCID$_{50}$ per ml) for another 36 h. Data were from three independent
529 experiments. Values are expressed as mean ± SEM and analyzed by Student's *t*-test (*$p < 0.05$, **$p < 0.01$, ***$p<$
530 0.001, ns non-significant). Source data are provided as a Source Data file.

531 **Figure 6. Bmp8a activates the IFN expression through Alk6a.** (**A, C**) Immunoblot analysis of phosphorylated
532 (p-) p38 MAPK after transfected with alk6a or empty vector in ZFL (**A**) or EPC (**C**) cells. The cells were collected
533 at 36 h or 48 h post transfection for Immunoblot analysis. (**B, D**) Immunoblot analysis of phosphorylated (p-) p38
534 MAPK after transfected with alk6a or empty vector in ZFL (**B**) or EPC (**D**) cells for 24 h, followed by infection with
535 GCRV (5 × 10^4TCID$_{50}$ per ml) for another 24 h or 36 h. (**E, G**) Immunoblot analysis of phosphorylated (p-) p38
536 MAPK after transfected with alk6a-ΔGS or empty vector in ZFL (**E**) or EPC (**G**) cells. The cells were collected at
537 36 h or 48 h post transfection for Immunoblot analysis. (**F, G**) Immunoblot analysis of phosphorylated (p-) p38
538 MAPK after transfected with alk6a or empty vector in ZFL (**F**) or EPC (**G**) cells for 24 h, followed by infection with
539 GCRV (5 × 10^4TCID$_{50}$ per ml) for another 24 h or 36 h. (**I**–**K**) EPC cells were cotransfected with pGL3-IFNφ1-
540 promoter-luc (**I**), pGL3-IFNφ3-promoter-luc (**J**) or pGL3-EPC IFN-promoter-luc (**K**), and bmp8a together with or
541 without the dominant negative plasmids alk6a-ΔGS. At 48 h post transfection, the cells were collected for luciferase
542 assays. *Renilla* luciferase was used as the internal control. **L** Co-immunoprecipitation and immunoblot analysis of
543 EPC cells cotransfected with alk6a-Flag and bmp8a-HA. Data were from three independent experiments. Values
544 are expressed as mean ± SEM and analyzed by Student's *t*-test (***$p<0.001$). Source data are provided as a
545 Source Data file.

546 **Figure 7. GCRV or poly(I:C) increases the expression of *bmp8a*.** (**A**) Expression of *bmp8a* mRNA in ZFL cells

547 after infected with GCRV (5 × 10^4TCID$_{50}$ per ml) for 48 h. (**B**–**E**) Expression of *bmp8a* mRNA in the liver (**B**), spleen
548 (**C**), intestine (**D**), and kidney (**E**) from zebrafish injected i.p. with poly(I:C) (10 μg/fish). (**F**–**I**) Expression of *bmp8a*
549 mRNA in the liver (**F**), spleen (**G**), intestine (**H**), and kidney (**I**) from zebrafish injected i.p. with 50μl of GCRV
550 (10^8TCID$_{50}$ per ml). Zebrafish injected i.p. with PBS or MEM were used as the control. The expression of *actb1*
551 served as a control for the qRT-PCR. Data were from three independent experiments. Values are expressed as
552 mean ± SEM and analyzed by Student's *t*-test (*p < 0.05, **p < 0.01, ***p < 0.001, ns non-significant). Source data
553 are provided as a Source Data file.

554 **Figure 8. Stat1 binds the GAS sites and activates the *bmp8a* transcriptions upon virus stimulation.** (**A, B**)
555 Expression of *bmp8a* mRNA in ZFL cells after transfected with stat1a-ΔC or stat1b-ΔC for 36 h (**A**) or 48 h (**B**). (**C**)
556 Dual luciferase report assay was used to analyze the transcription abilities of Stat1a and Stat1b in activation of
557 *bmp8a* in EPC cells. pGl3-bmp8a-promoter-luc was transfected into EPC cells together with stat1a, stat1b or
558 empty vector. After 48 h, the transfected cells were collected for luciferase assays. (**D**) Schematic drawing of wild-
559 type and GAS motif mutation Luc-report plasmids. (**E**) The pGL3-bmp8a-promoter, pGL3-bmp8a-promoter-ΔP1,
560 pGL3-bmp8a-promoter-ΔP2 or pGL3-bmp8a-promoter-ΔP1 and ΔP2 was transfected into EPC cells along with
561 stat1a, stat1b or empty vector, respectively. After 48 h, the transfected cells were collected for luciferase assays.
562 *Renilla* luciferase was used as the internal control. Data were from three independent experiments. Values are
563 expressed as mean ± SEM and analyzed by Student's *t*-test (**p < 0.01, ***p < 0.001). (**F**, **G**) SDS-PAGE and
564 Western-blotting analysis of rStat1a (**F**) and rStat1b (**G**). Lane M: protein molecular standard; Lane 1: negative
565 control for IPTG induced *E. coli* (without rStat1a or rStat1b); Lane2: induced rStat1a or rStat1b (the whole cell
566 lysate); Lane 3: induced rStat1a or rStat1b (the supernatant); Lane 4: purified rStat1a or rStat1b; Lane 5: western
567 blot analysis of the sample in Lane 4. (**H**–**K**) EMSA was performed to validate the interaction of rStat1a or rStat1b
568 with the GAS motif (P1 or P2) in the bmp8a promoter region. Lane 1: negative group; Lane 2: positive group; Lane
569 3: an excess unlabeled competitor probe; Lane 4: an excess unlabeled competitor probe containing a mutated
570 runt binding site; Lane 5: Super-shift assays were performed by adding antibody against His tag. Source data are
571 provided as a Source Data file.

572 **Figure 9. Schematic illustration of Bmp8a serving as positive regulator in the antiviral immune**. Upon virus
573 infection, the transcriptions of *bmp8a* are activated through the Jak-Stat1 pathway. The Bmp8a binds to BMP type
574 I receptor Alk6a, promoting phosphorylation of Tbk1 and Irf3 to induce the expression of *Ifn* through p38 MAPK
575 pathway.

576

577 **Figure 1 – Figure supplement 1. Generation of zebrafish *bmp8a* mutant alleles using TALENs technology**.

578 (**A**) Partial structure and sequence of the *bmp8a* gene, showing the binding sites (underlined) of the left and right

579 TALENs. (**B**) Sequences of *bmp8a* homozygous mutant. Deletions of 7 bp are indicated by dashes letters. The

580 sequences of *bmp8a* in wild type (WT) zebrafish were used as a control. (**C**) Bmp8a in WT, 434 amino acids (aa)

581 long, contains a TGFβ-propeptide domain (yellow) and a TGFβ domain (green). The *bmp8a*$^{-/-}$ encodes a truncated

582 281-amino-acid-long polypeptide that contains a partial TGFβ-propeptide domains (yellow) followed by a

583 frameshift leading to a premature stop codon.

584 **Figure 1 – Figure supplement 2. A new virus (TSVDV) was isolated from the focal site of turbot skin.** (**A**)

585 Skin ulceration appeared on the skin surface (green arrow) of turbot infected with TSVDV (***Qin et al., 2008***). (**B**)

586 The FG cells had obvious cytopathic effect (CPE) after TSVDV infection.

587 **Figure 3 – Figure supplement 1. Kyoto Encyclopedia of Genes and Genomes (KEGG) analysis of the top**

588 **10 pathways by enrichment of differential expressed genes (DEGs) between *bmp8a*$^{-/-}$ and WT liver tissue**

589 **of zebrafish challenged by GCRV.** Rich ratio is the ratio of differentially expressed gene numbers annotated in

590 this pathway terms to all gene numbers annotated in this pathway term. The *q*-value means corrected p-value, q

591 < 0.05 as significantly enriched.

592 **Figure 8 – Figure supplement 1. Sequence analysis of *bmp8a* promoter region.** Two GAS motifs (P1 and P2)

593 have been found in the *bmp8a* promoter region, which were underlined. The transcriptional start site was

594 designated by +1.

595

596

597

598

599

600

601

602

603

604

605

606

607 **References**

608 Thaiss, C. A., Levy, M., Itav, S. & Elinav, E. Integration of Innate Immune Signaling. *Trends Immunol*. **37**, 84-101

609 (2016).

610 Akira, S. & Hemmi, H. Recognition of pathogen-associated molecular patterns by TLR family. *Immunol*. *Lett*. **85**,

611 85-95 (2003).

612 Chen, S. N., Zou, P. F. & Nie, P. Retinoic acid-inducible gene I (RIG-I)-like receptors (RLRs) in fish: current

613 knowledge and future perspectives. *Immunology* **151**, 16-25 (2017).

614 Keating, S. E., Baran, M. & Bowie, A. G. Cytosolic DNA sensors regulating type I interferon induction. *Trends*

615 *Immunol*. **32**, 574-581 (2011).

616 Parvatiyar, K. et al. The helicase DDX41 recognizes the bacterial secondary messengers cyclic di-GMP and cyclic

617 di-AMP to activate a type I interferon immune response. *Nat*. *Immunol*. **13**, 1155-1161 (2012).

618 Honda, K. et al. IRF-7 is the master regulator of type-I interferon-dependent immune responses. *Nature* **434**, 772-

619 777 (2005).

620 Tamura, T., Yanai, H., Savitsky, D. & Taniguchi, T. The IRF family transcription factors in immunity and oncogenesis.

621 *Annu*. *Rev*. *Immunol*. **26**, 535-584 (2008).

622 Li, W., Hofer, M. J., Jung, S. R., Lim, S. L. & Campbell, I. L. IRF7-dependent type I interferon production induces

623 lethal immune-mediated disease in STAT1 knockout mice infected with lymphocytic choriomeningitis virus. *J*. *Virol*.

624 **88**, 7578-7588 (2014).

625 Schindler, C. & Plumlee, C. Inteferons pen the JAK-STAT pathway. *Semin*. *Cell Dev*. *Biol*. **19**, 311-318 (2008).

626 Decker, T., Kovarik, P. & Meinke, A. GAS elements: a few nucleotides with a major impact on cytokine-induced

627 gene expression. *J*. *Interferon Cytokine Res*. **17**, 121-134 (1997).

628 Fu, X. Y., Kessler, D. S., Veals, S. A., Levy, D. E. & Darnell, J. E. Jr. ISGF3, the transcriptional activator induced

629 by interferon alpha, consists of multiple interacting polypeptide chains. *Proc*. *Natl Acad*. *Sci*. *USA* **87**, 8555-8559

630 (1990).

631 Levy, D. E., Kessler, D. S., Pine, R. & Darnell, J. E. Jr. Cytoplasmic activation of ISGF3, the positive regulator of

632 interferon-alpha-stimulated transcription, reconstituted in vitro. *Genes Dev*. **3**, 1362-1371 (1989).

633 Levy, D. E., Kessler, D. S., Pine, R., Reich, N. & Darnell, J. E. Jr. Interferon-induced nuclear factors that bind a

634 shared promoter element correlate with positive and negative transcriptional control. *Genes Dev*. **2**, 383-393

635 (1988).

636 Ren, Y. et al. Deubiquitinase USP2a Sustains Interferons Antiviral Activity by Restricting Ubiquitination of Activated

637 STAT1 in the Nucleus. *PLoS Pathog*. **12**, e1005764 (2016).

638 Shuai, K., Schindler, C., Prezioso, V. R. & Darnell, J. E. Jr. Activation of transcription by IFN-gamma: tyrosine

639 phosphorylation of a 91-kD DNA binding protein. *Science* **258**, 1808-1812 (1992).

640 Bragdon, B., Moseychuk, O., Saldanha, S., King, D., Julian, J. & Nohe, A. Bone morphogenetic proteins: a critical

641 review. *Cell Signal* **23**, 609-620 (2011).

642 Wu, M., Chen, G. & Li, Y. P. TGF-beta and BMP signaling in osteoblast, skeletal development, and bone formation,

643 homeostasis and disease. *Bone Res*. **4**, 16009 (2016).

644 Huber, S. & Schramm, C. Role of activin A in the induction of Foxp3+ and Foxp3- CD4+ regulatory T cells. *Crit*.

645 *Rev*. *Immunol*. **31**, 53-60 (2011).

646 Martínez, V. G. et al. The canonical BMP signaling pathway is involved in human monocyte-derived dendritic cell

647 maturation. *Immunol*. *Cell Biol*. **89**, 610-618 (2011).

648 Martínez, V. G. et al. The BMP Pathway Participates in Human Naive CD4+ T Cell Activation and Homeostasis.

649 *PloS One* **10**, e0131453 (2015).

650 Phillips, D. J., de Kretser, D. M. & Hedger, M. P. Activin and related proteins in inflammation: not just interested

651 bystanders. *Cytokine Growth Factor Rev*. **20**, 153-164 (2009).

652 Seeger, P., Musso, T. & Sozzani, S. The TGF-β superfamily in dendritic cell biology. *Cytokine Growth Factor Rev*.

653 **26**, 647-657 (2015).

654 Takabayashi, H. et al. Anti-inflammatory activity of bone morphogenetic protein signaling pathways in stomachs of

655 mice. *Gastroenterology* **147**, 396-406 (2014).

656 Yasmin, N. et al. Identification of bone morphogenetic protein 7 (BMP7) as an instructive factor for human

657 epidermal Langerhans cell differentiation. *J*. *Exp*. *Med*. **210**, 2597-2610 (2013).

658 Sivertsen, E. A., Huse, K., Hystad, M. E., Kersten, C., Smeland, E. B. & Myklebust, J. H. Inhibitory effects and

659 target genes of bone morphogenetic protein 6 in Jurkat TAg cells. *Eur*. *J*. *Immunol*. **37**, 2937-2948 (2007).

660 Varas, A. et al. Interplay between BMP4 and IL-7 in human intrathymic precursor cells. *Cell cycle* **8**, 4119-4126

661 (2009).

662 Chen, W. & Ten Dijke, P. Immunoregulation by members of the TGFβ superfamily. *Nat*. *Rev*. *Immunol*. **16**, 723-

663 740 (2016).

664 Zhao, G. Q. & Hogan, B. L. Evidence that mouse Bmp8a (Op2) and Bmp8b are duplicated genes that play a role

665 in spermatogenesis and placental development. *Mech*. *Dev*. **57**, 159-168 (1996).

666 Walton, K. D. et al. Villification in the mouse: Bmp signals control intestinal villus patterning. *Development* **143**,

667 427-436 (2016).

668 Ying, Y., Qi, X. & Zhao, G. Q. Induction of primordial germ cells from murine epiblasts by synergistic action of
669 BMP4 and BMP8B signaling pathways. *Proc*. *Natl Acad*. *Sci*. *USA* **98**, 7858-7862 (2001).

670 Zhong, S. j. et al. Spatial and temporal expression of *bmp8a* and its role in regulation of lipid metabolism in
671 zebrafish *Danio rerio*. *Gene Rep*. **10**, 33-41 (2018).

672 Robertsen, B. The interferon system of teleost fish. *Fish Shellfish Immunol*. **20**, 172-191 (2006).

673 Zhang, Y. B. et al. The innate immune response to grass carp hemorrhagic virus (GCHV) in cultured Carassius
674 auratus blastulae (CAB) cells. *Dev*. *Comp*. *Immunol*. **31**, 232-243 (2007).

675 Derynck, R., Akhurst, R. J. & Balmain, A. TGF-beta signaling in tumor suppression and cancer progression. *Nat*.
676 *Genet*. **29**, 117-129 (2001).

677 Drummond, A. E. TGFbeta signalling in the development of ovarian function. *Cell Tissue Res*. **322**, 107-115 (2005).

678 Oh, S. P., Yeo, C. Y., Lee, Y., Schrewe, H., Whitman, M. & Li, E. Activin type IIA and IIB receptors mediate Gdf11
679 signaling in axial vertebral patterning. *Genes Dev*. **16**, 2749-2754 (2002).

680 Shi, Y. et al. Exosomal Interferon-Induced Transmembrane Protein 2 Transmitted to Dendritic Cells Inhibits
681 Interferon Alpha Pathway Activation and Blocks Anti-Hepatitis B Virus Efficacy of Exogenous Interferon Alpha.
682 *Hepatology* **69**, 2396-2413 (2019).

683 Heldin, C. H., Miyazono, K. & ten Dijke, P. TGF-beta signalling from cell membrane to nucleus through SMAD
684 proteins. *Nature* **390**, 465-471 (1997).

685 Shi, Y. & Massagué, J. Mechanisms of TGF-beta signaling from cell membrane to the nucleus. *Cell* **113**, 685-700
686 (2003).

687 Worthington, J. J., Fenton, T. M., Czajkowska, B. I., Klementowicz, J. E. & Travis, M. A. Regulation of TGFβ in the
688 immune system: an emerging role for integrins and dendritic cells. *Immunobiology* **217**, 1259-1265 (2012).

689 Tu, E., Chia, P. Z. & Chen, W. TGFβ in T cell biology and tumor immunity: Angel or devil? *Cytokine Growth Factor*
690 *Rev*. **25**, 423-435 (2014).

691 Aleman-Muench, G. R. & Soldevila, G. When versatility matters: activins/inhibins as key regulators of immunity.
692 *Immunol. Cell Biol*. **90**, 137-148 (2012).

693 Bleul, C. C. & Boehm, T. BMP signaling is required for normal thymus development. *J*. *Immunol*. **175**, 5213-5221
694 (2005).

695 Gordon, J., Patel, S. R., Mishina, Y. & Manley, N. R. Evidence for an early role for BMP4 signaling in thymus and
696 parathyroid morphogenesis. *Dev*. *Biol*. **339**, 141-154 (2010).

697 Lee, M. K. et al. TGF-beta activates Erk MAP kinase signalling through direct phosphorylation of ShcA. *EMBO J*.
698 **26**, 3957-3967 (2007).
699 Itoh, S. et al. Trps1 plays a pivotal role downstream of Gdf5 signaling in promoting chondrogenesis and apoptosis
700 of ATDC5 cells. *Genes Cells* **13**, 355-363 (2008).
701 Wu, H., Zhang, Y., Lu, X., Xiao, J., Feng, P. & Feng, H. STAT1a and STAT1b of black carp play important roles in
702 the innate immune defense against GCRV. *Fish Shellfish Immunol*. **87**, 386-394 (2019).
703 Zou, J. & Secombes, C. J. Teleost fish interferons and their role in immunity. *Dev*. *Comp*. *Immunol*. **35**, 1376-1387
704 (2011).
705 Ruan, B. Y. et al. Two type II IFN members, IFN-γ and IFN-γ related (rel), regulate differentially IRF1 and IRF11 in
706 zebrafish. *Fish Shellfish Immunol*. **65**, 103-110 (2017).
707 Boehm, U., Klamp, T., Groot, M. & Howard, J. C. Cellular responses to interferon-gamma. *Annu. Rev*. *Immunol*.
708 **15**, 749-795 (1997).
709 Reed, L. J. & Muench, H. A Simple Method of Estimating Fifty Percent Endo-Points. *Am*. *J*. *Hyg*. **27**, 493-797
710 (1938).
711 Huang, P., Xiao, A., Tong, X., Zu, Y., Wang, Z. & Zhang, B. TALEN construction via "Unit Assembly" method and
712 targeted genome modifications in zebrafish. *Methods* **69**, 67-75 (2014).
713 Feng, H., Zhang, Y. B., Zhang, Q. M., Li, Z., Zhang, Q. Y. & Gui, J. F. Zebrafish IRF1 regulates IFN antiviral
714 response through binding to IFNϕ1 and IFNϕ3 promoters downstream of MyD88 signaling. *J*. *Immunol*. **194**, 1225-
715 1238 (2015).
716 Sun, F., Zhang, Y. B., Liu, T. K., Shi, J., Wang, B. & Gui, J. F. Fish MITA serves as a mediator for distinct fish IFN
717 gene activation dependent on IRF3 or IRF7. *J*. *Immunol*. **187**, 2531-2539 (2011).
718 Mortazavi, A., Williams, B. A., McCue, K., Schaeffer, L. & Wold, B. Mapping and quantifying mammalian
719 transcriptomes by RNA-Seq. *Nat*. *Methods* **5**, 621-628 (2008).
720 Sun, C., Hu, L., Liu, S., Gao, Z. & Zhang, S. Functional analysis of domain of unknown function (DUF) 1943,
721 DUF1944 and von Willebrand factor type D domain (VWD) in vitellogenin2 in zebrafish. *Dev*. *Comp*. *Immunol*. **41**,
722 469-476 (2013).
723 Qin, L., Wang. Y. G. & Zhang, Z. Multiple verrucous protrusions on skin in turbot Scophthalmus maximus. *J*. *Dalian*
724 *Ocean Univ*. **23**, 479-483 (2008) (in Chinese with English abstract).
725
726
727
728

729 **Figure 1**

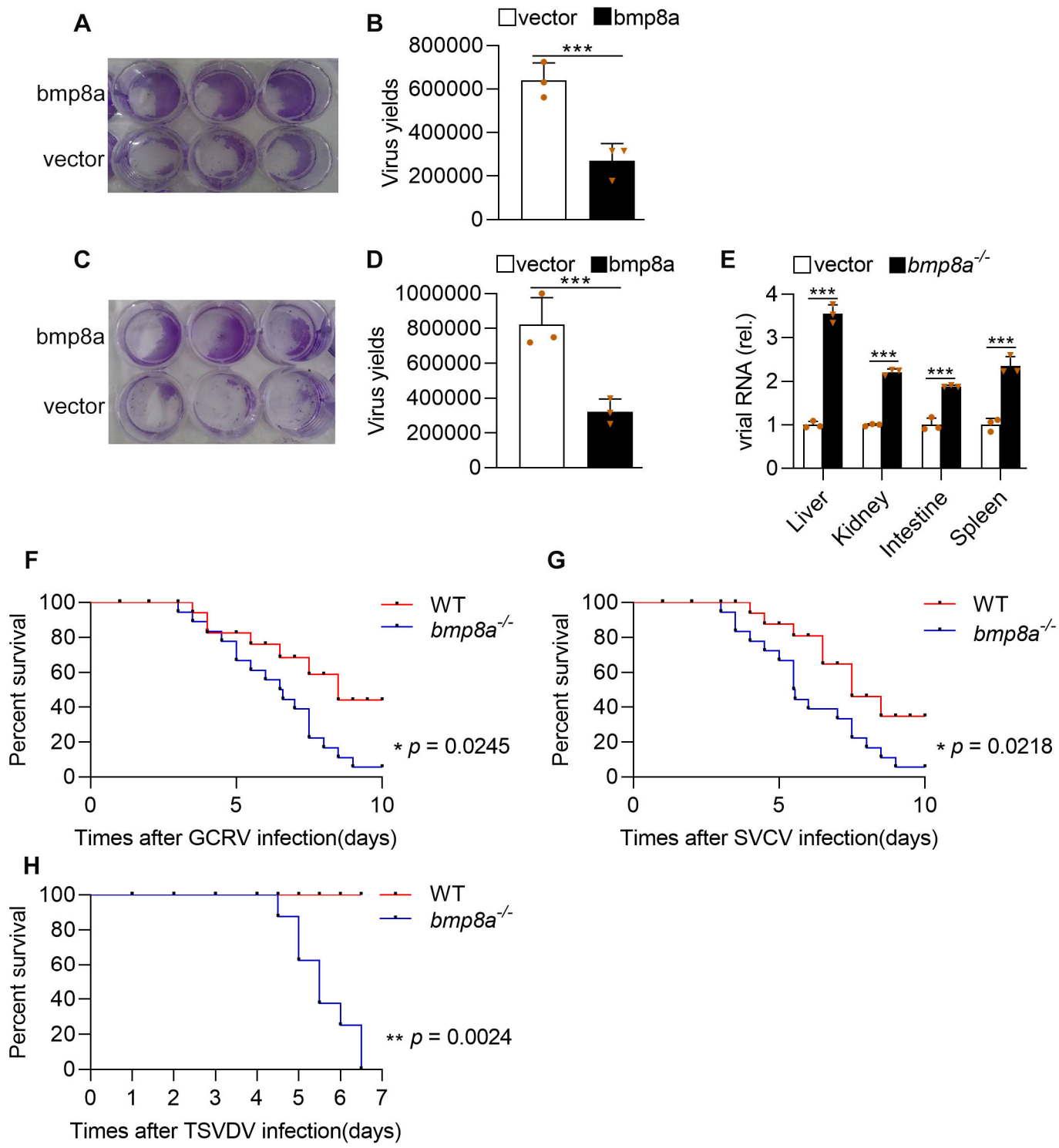

730

731

732

733

734

735

736

737

738

739

740

741 **Figure 2**

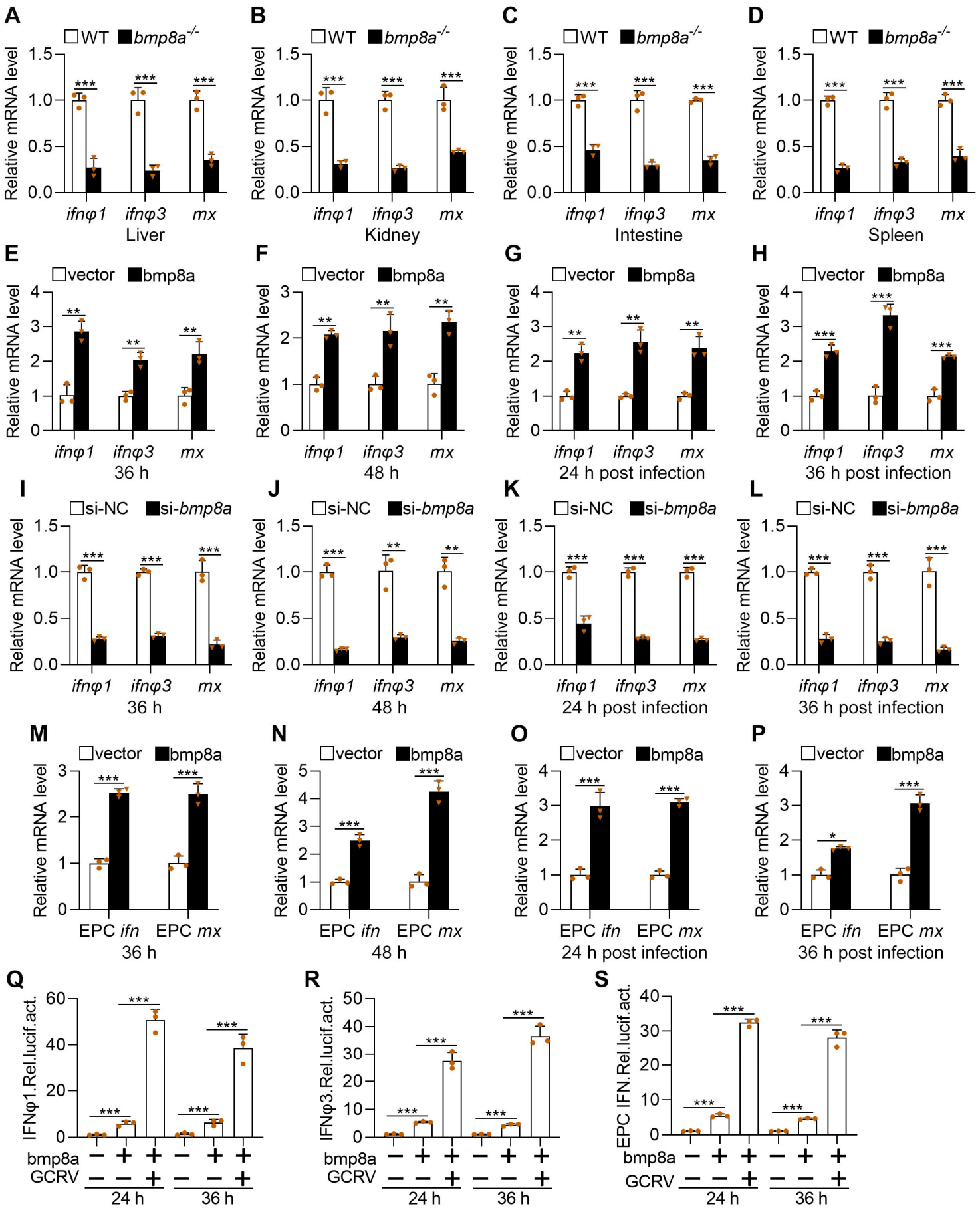

742

743

744

745

746

747

748

749

750 **Figure 3**

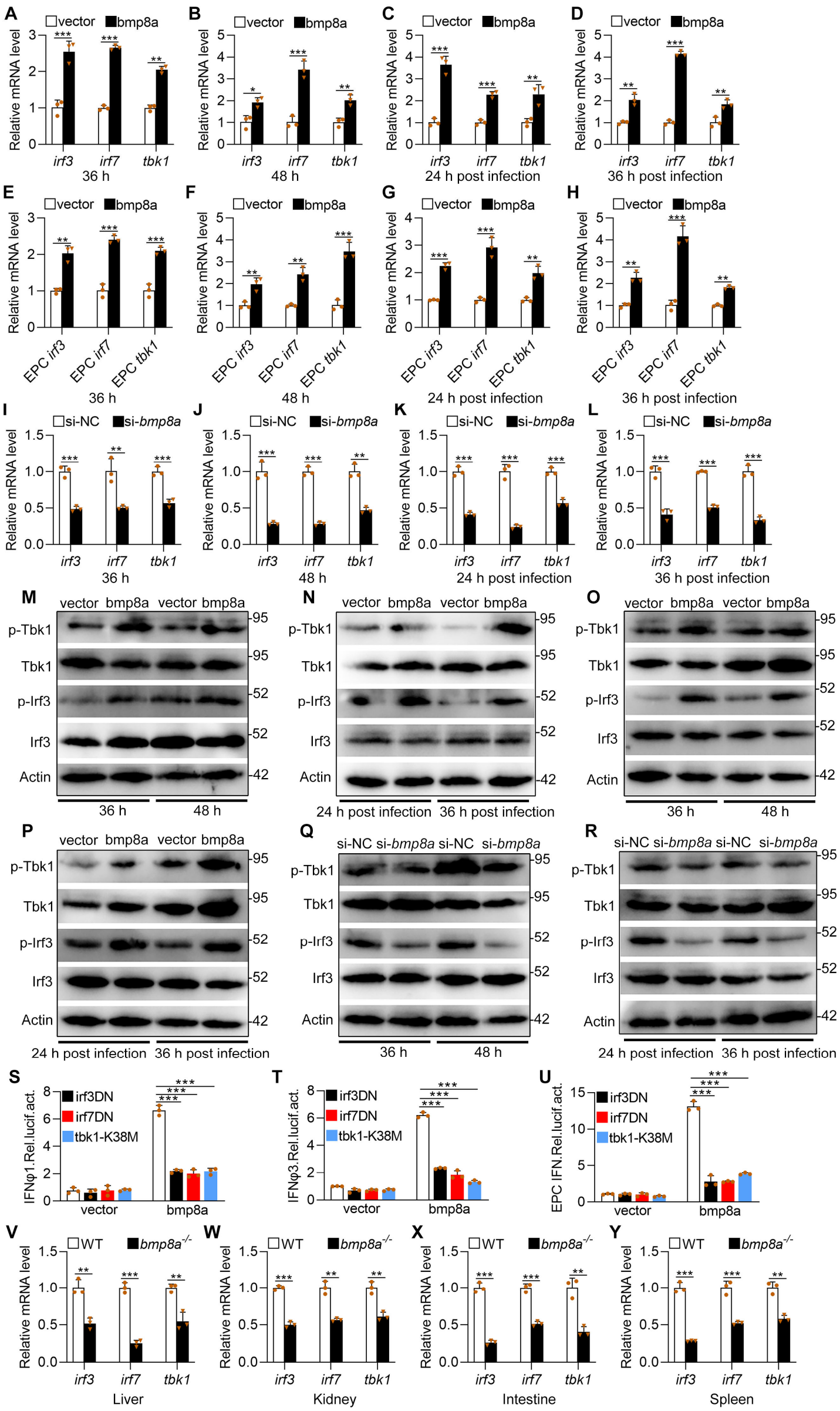

751

752 **Figure 4**

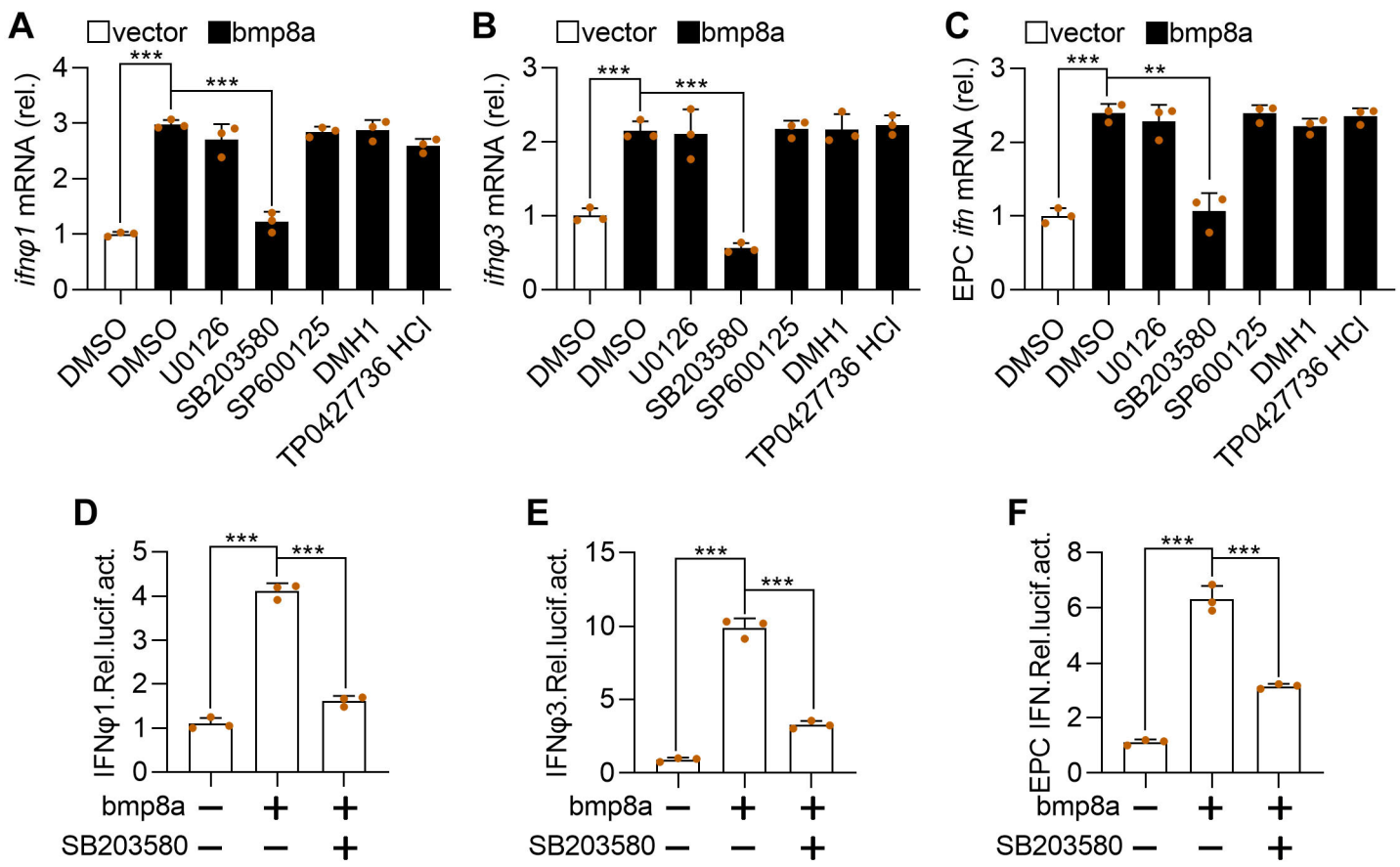

753

754

755

756

757

758

759

760

761

762

763

764

765

766

767

768

769

770

771 **Figure 5**

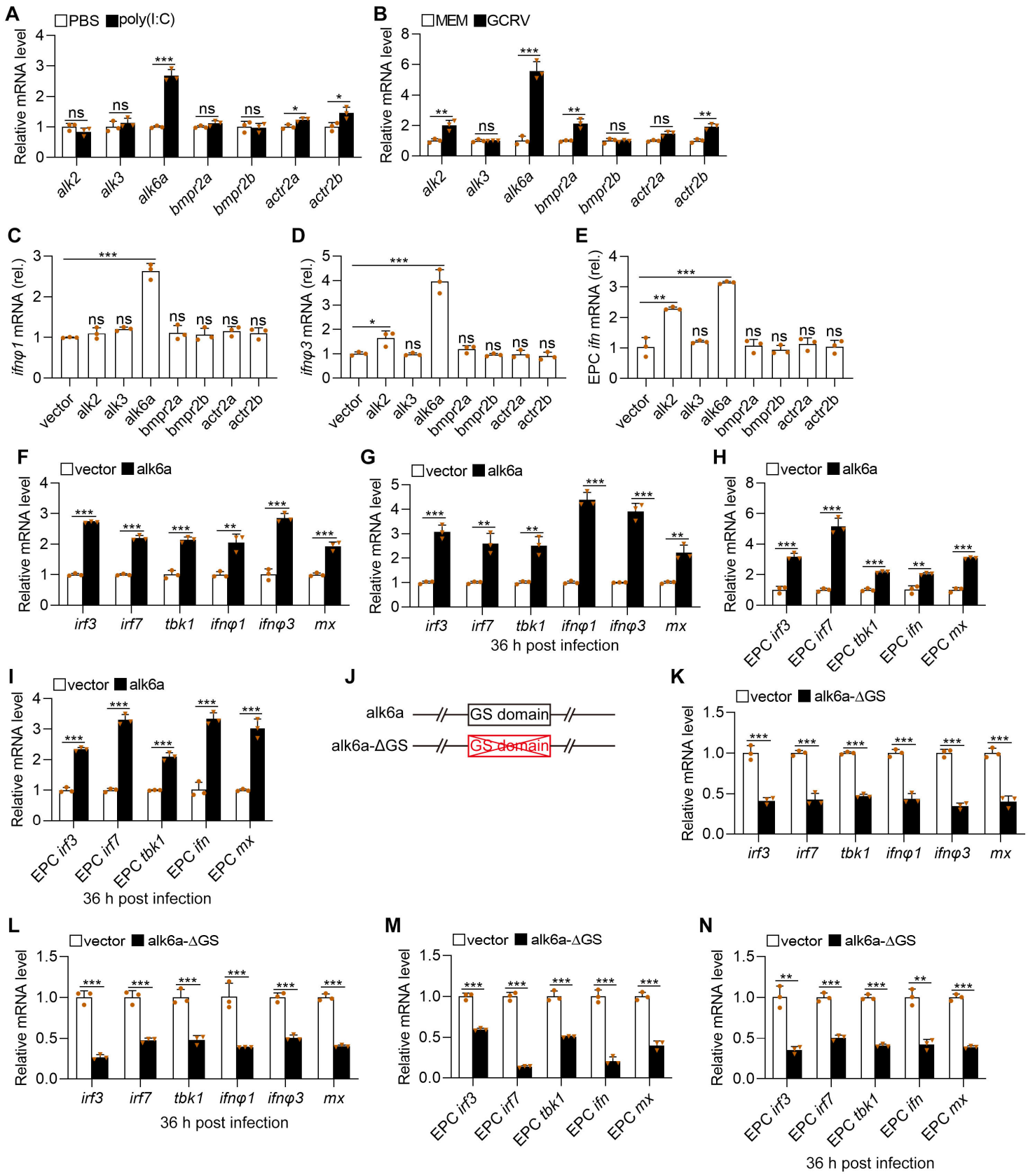

772

773

774

775

776

777

778

779

780

781 **Figure 6**

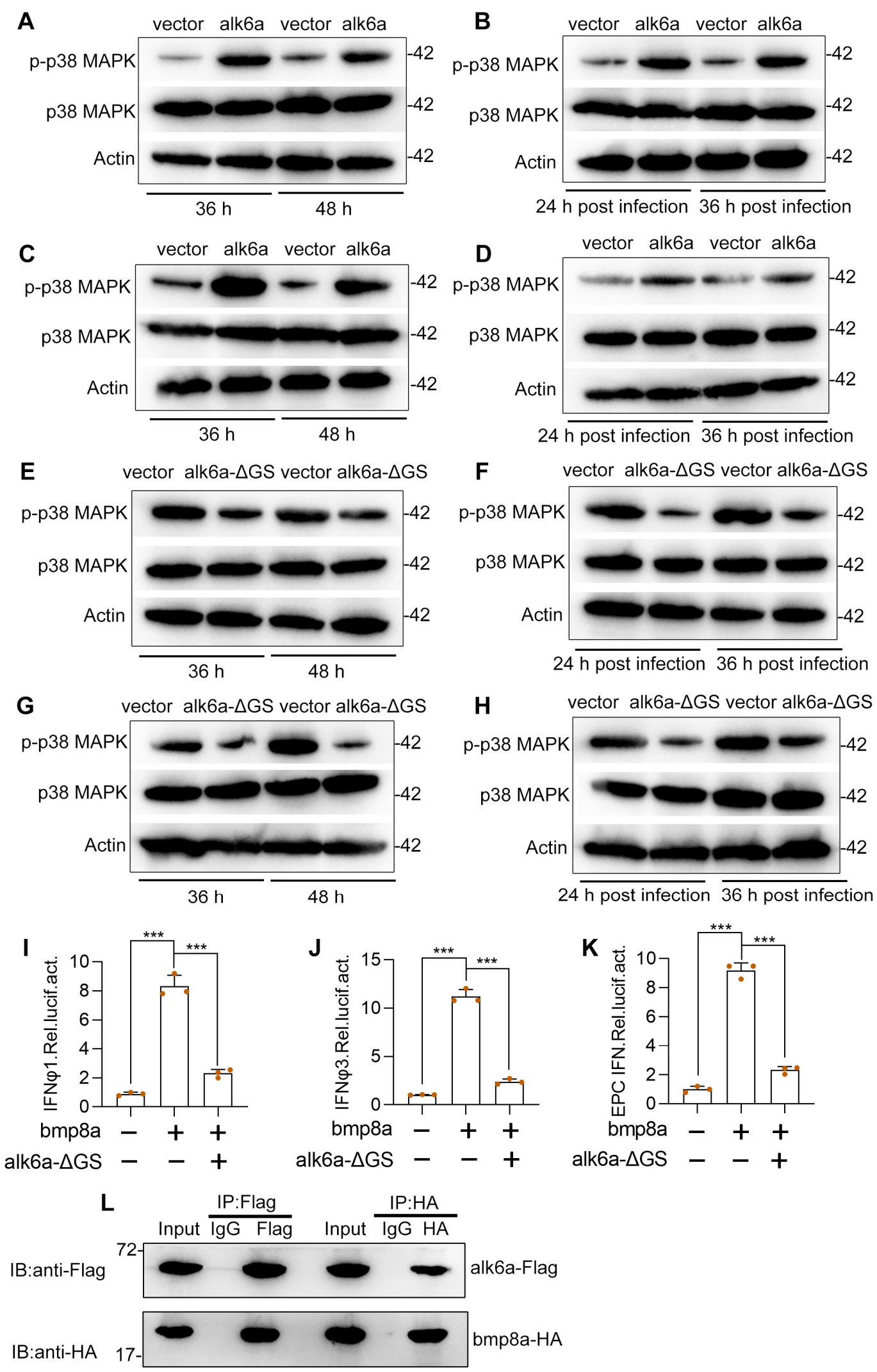

782

783

784

785 **Figure 7**

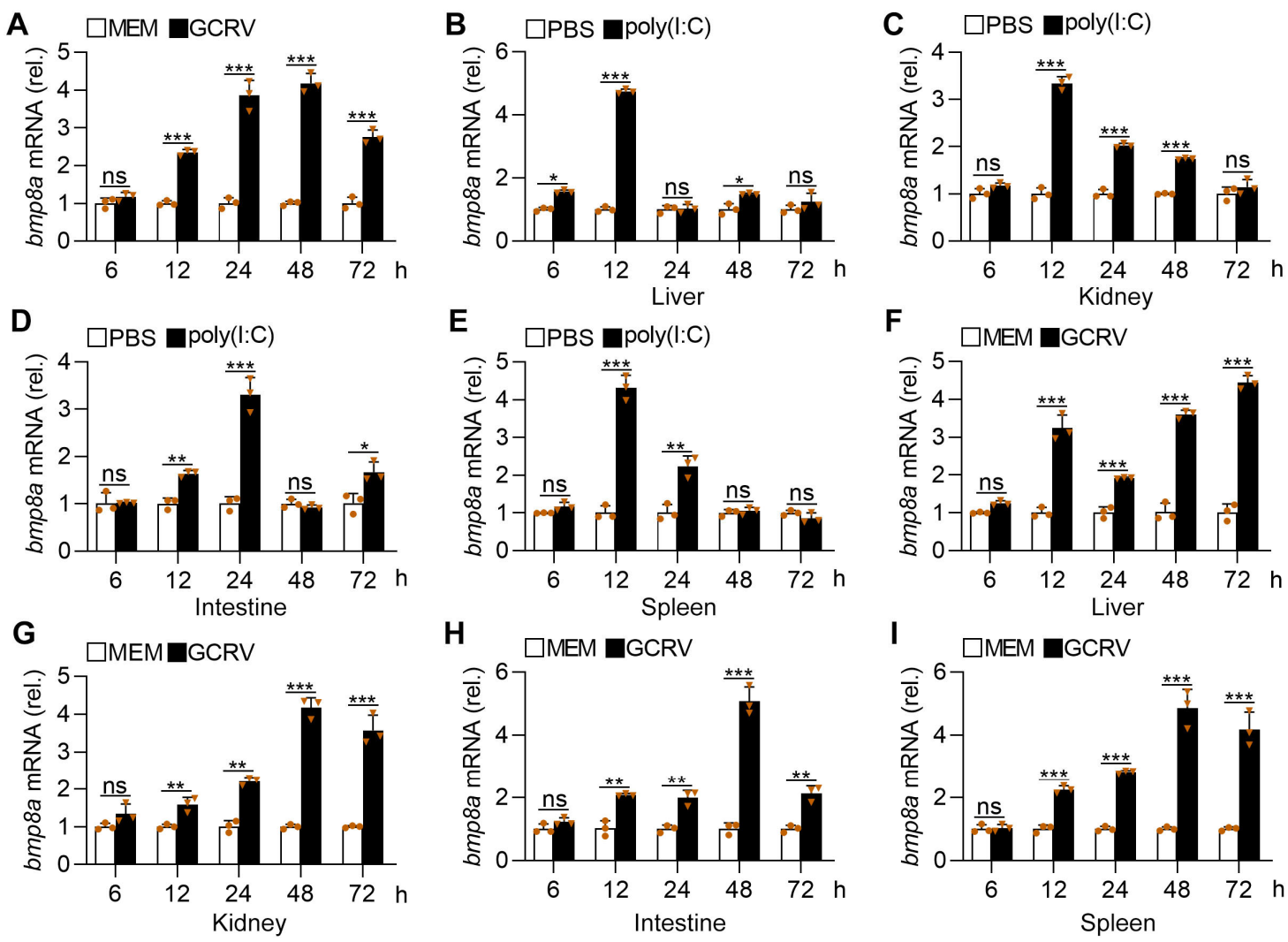

786

787

788

789

790

791

792

793

794

795

796

797

798

799

800

801

802 **Figure 8**

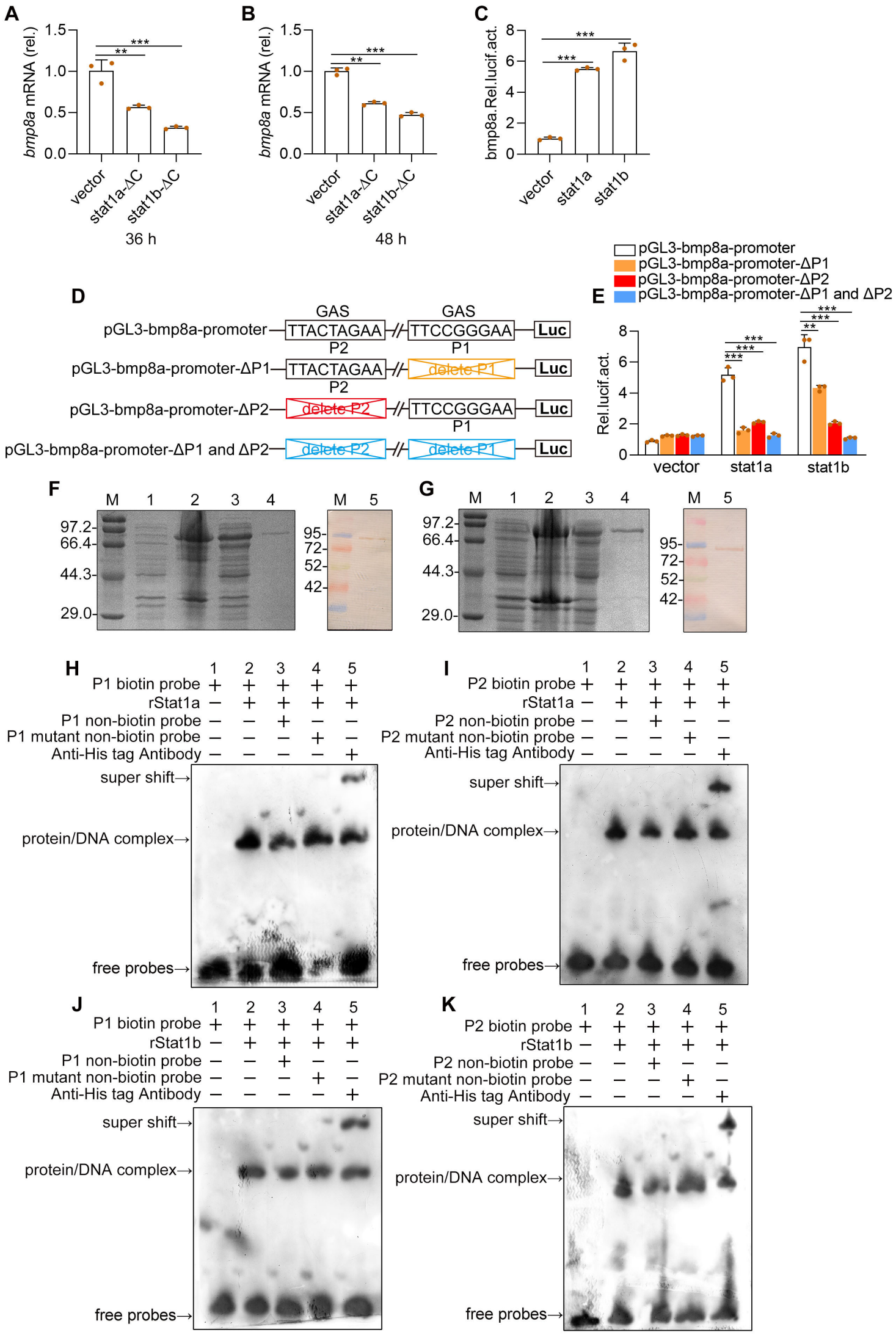

803

804

Figure 9

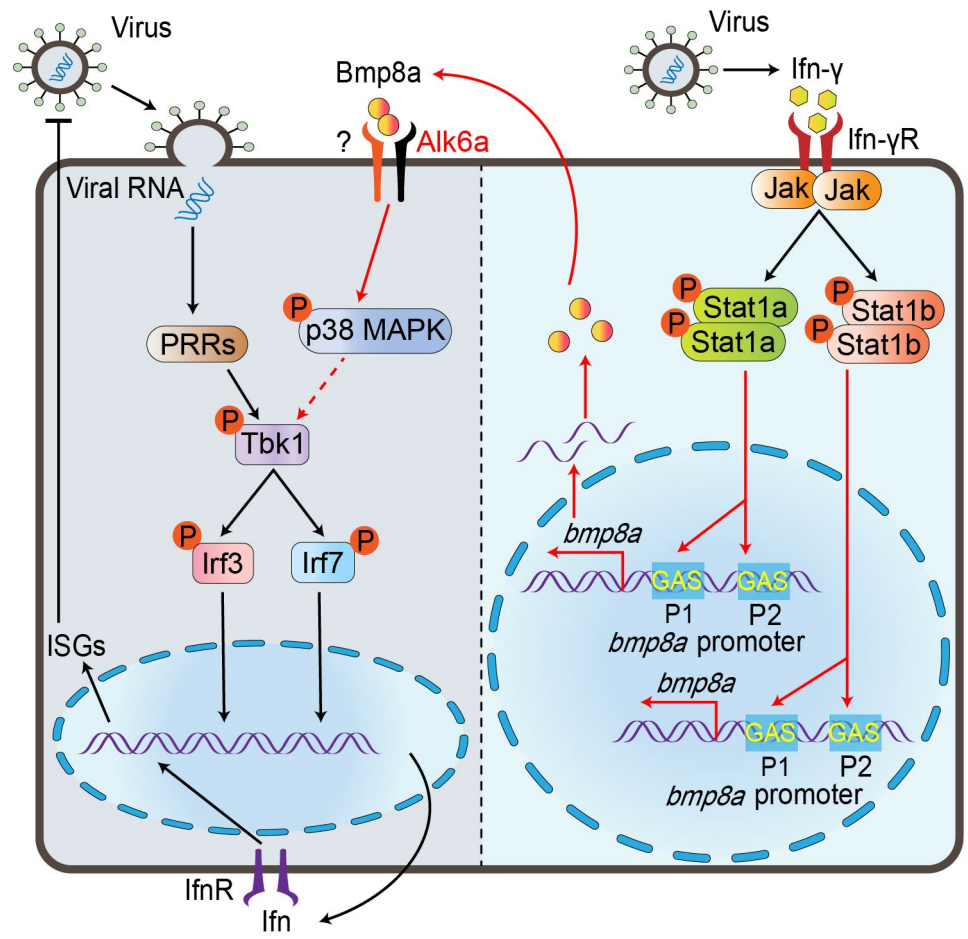
Virus
Bmp8a
Virus
Ifn-γ
?
Alk6a
Ifn-γR
Viral RNA
Jak
Jak
P
p38 MAPK
P
Stat1a
P
Stat1a
P
Stat1b
P
Stat1b
PRRs
P
Tbk1
bmp8a
P
Irf3
Irf7
P
GAS
GAS
P1
P2
bmp8a promoter
ISGs
bmp8a
GAS
GAS
P1
P2
bmp8a promoter
IfnR
Ifn

824 **Figure 1 – Figure supplement 1**

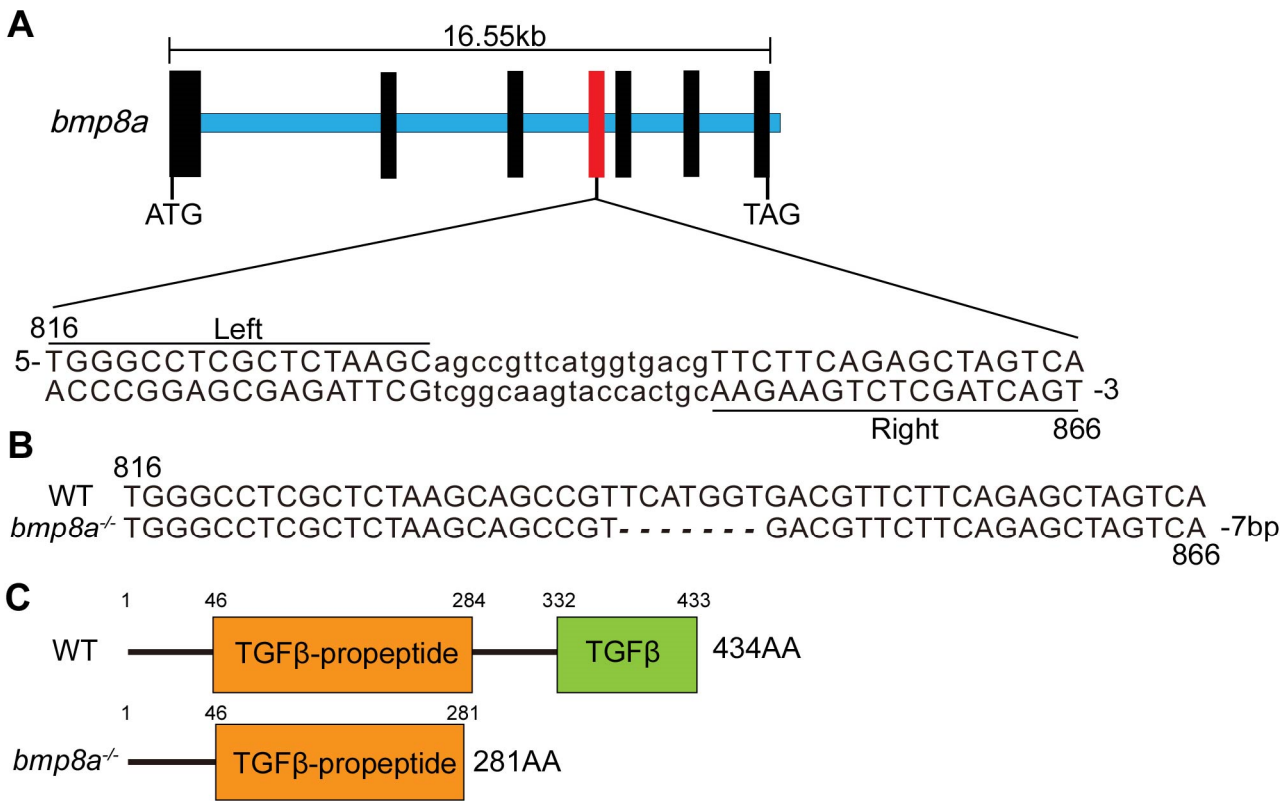

825

826

827 **Figure 1 – Figure supplement 2**

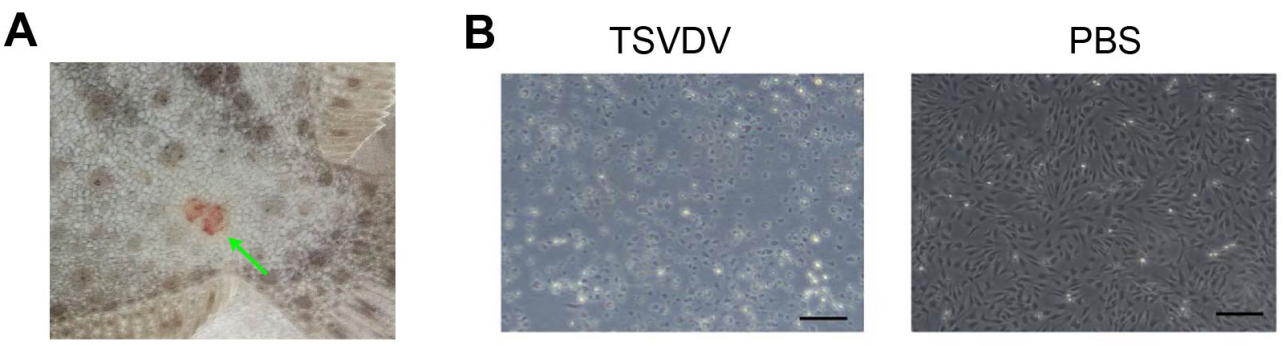

828

829

830 **Figure 3 – Figure supplement 1**

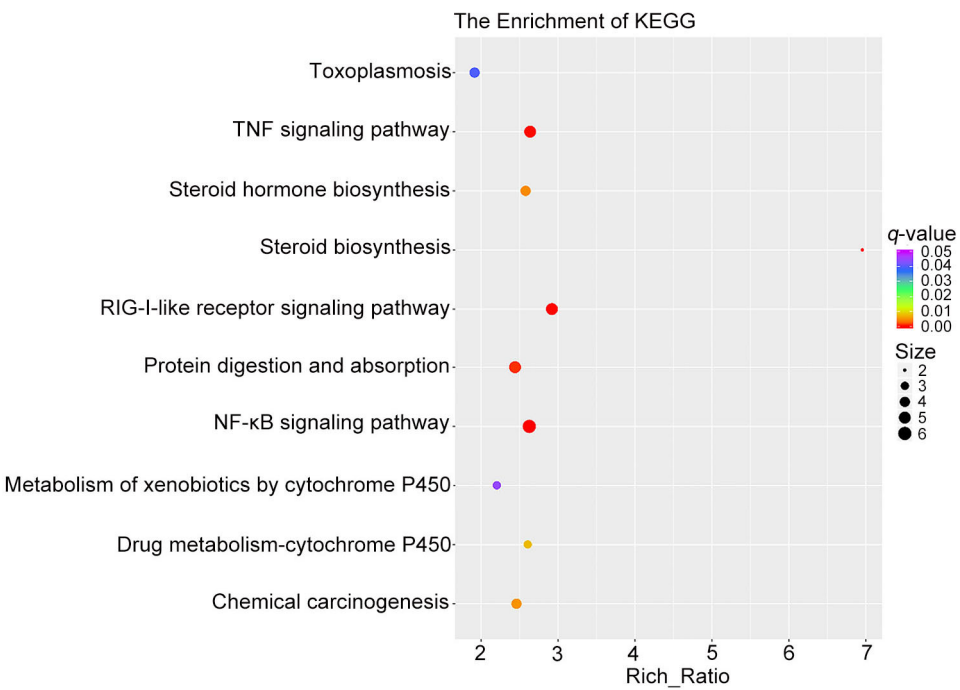

831

832 **Figure 8 – Figure supplement 1**

```
-1439 TCACTTTCGTCAATTGGTGAAGTTTGTTCCTCATGACTGGCTTGCTTGGTTTGGGACTTGTGGAGCT
-1372 GCGCATCGATGGATTTGTTCTTCAGTGTTTGGACTTTCAGTAGGGAAAATTAAACC
                                                   GAS motif
-1316 ACACTGAACTGAACTTCAACTCTGAAAACTGGTCTGACTCCGTTTCAATTTACTAGAACTT
                                                         P2
-1255 CTCTGTTAAGCTGATCTGACACAATCTACATTGTAAAAGTGCTATAGAAATAAAGATGAAATAAATT
-1188 TTTATAATATTTACCTAAGTACACTGCTCCAAAAAATAAAGGGAACACTTAAACAACACAATATAA
-1122 CCATGTGTTGCCTTTATCTTTTTAGCAGTATGTTTATGCATTTGGTGCTGTAATGAACAACTACTAAT
-1054 ATAACAATCTGAATATTCCTAACAGCCACTCTAAAAGTTTAAATAATATATTTTCAAGTGCACACGA
 -987 TATCAGTATTGTCACTATCACAATACATTGAATTGTTGAGTATCAACATACGTCTCATACACAGTGA
 -920 TCTCTCACTGCTTGGCTACCGCTGAACCCACAGAATACAAATTTAGTTTTCATATTACTGTAGCCAC
 -853 ACAAACTCCGTCCCATTCTGTGCAAAGACTGGATCACATCTCCACTCCAAACCACATGATAATTGT
 -787 CAGCAATTTGTGAGGTATGTGTAGAAGATGAGACGGTTTGATAGGGCAGATGGAGACTGAGGTGA
 -722 GAAGGGTTCAGGATAGAGAAAAGGGCGGAGGTTTGAGATGATGGAAACCCTCCCTCTGCGTAAG
 -658 CCTGTTTCTTGGAGGGAAGGAGCTCGCCTGTGTTCAGAGTAACCCTCCAGCGCAAGCAGCACACA
 -593 AGCTAAGAATACCACAGCTCAACAAAGTTCAGCGGTGAACCAATACAATTCCTTCTCAGAGTTTTC
 -527 AGGAGCCTTGGATTTTCCATCCTTTGGATTATTTGTTTTTTTTTTTAAAGCTCAACTTTTCATGGATTA
 -458 CCTCAAGACAGTTTTGTTTTTCAATTAAACAGAGGATTTCACCAGTGAAGAGTTCTCAAAAGAAGC
 -392 AGGTGTGCTTTTTAAAGGTTGACCGCTGTTTTTAGTTACTCTACCCAAAGACTTTCCATTCAACATT
 -325 GTGCTTTGTCCTTCCAACATCCAAAATCCAGTTTCCAGGATATATTGTCATCCATCTTTGTAAGTGC
 -258 ACTATAAATTATGAGATTGCTTTGGTAAATAAAGTGACGGCATGAGGAACGACTGTCAAGAGGCG
 -193 ATAAACTGAGCAAGTAAACATTGCACTCTTCCAAATAACGATGACTGCTGTGGAATCTGAGTGGCT
                                                      GAS motif
 -127 TAGACGTTCGAGTGTTGTTCGGGGTTGAACTTCGAGACGGTAGTCAGACCATTCCGGGAAAACCA
                                                          P1
  -62 ACGTCGGGTGAACAGCTAAAAGGACAAATATCTTTACAGACGGCTGGGCTCTTCGCTACACCA
      +1
    1 ATGGACAGACACGAGGTT
```

833

834

835

836

837

838

839

840

841

842

843

844

845

846 **Supplementary Table 1**

Primer names	Sequences (5' to 3')	Applications
irf3-F	GCTGTTCGTGCCCTGGTTGTATG	qRT-PCR for zebrafish
irf3-R	GCACATCGTCGCTGTTGGAGTC	
irf7-F	GCTGGAATTGCTCAACTTGGTGG	
irf7-R	CAGTCTGTGGTCGGGAAGCGTAT	
mx-F	CCTGGCAGAATCTATGCTGAAAAC	
mx-R	AAGGCAGTTTTATTTTCGGTTGTG	
ifnφ1-F	GTGGAGGACCAGGTGAAGTT	
ifnφ1-R	GATTGACCCTTGCGTTGC	
ifnφ3-F	TCTATACCATTCCCGCAAAA	
ifnφ3-R	GGATCACCGAAGTTCTCAAAC	
tbk1-F	TGATTGGAGACGACGGATTC	
tbk1-R	CCACTCGATCTTCCCATTTTC	
alk2-F	TGGGTTGGTGCTGTGGGAGA	
alk2-R	CGGGTGAGCGGTCAGTAGTT	
alk3-F	GCATCACGCTTAACCATCC	
alk3-R	TCCCAAATCCACCAGAACA	
alk6a-F	AGTGTCTCCGACAGATGGGG	
alk6a-R	TGTGAGTTCAGGGTTTGGGT	
bmpr2a-F	GAGATACCAAAACTCGACCCG	
bmpr2a-R	TCCTTGTGACCCCGAAACC	
bmpr2b-F	GTGATGATGGGCGAGTGTAA	
bmpr2b-R	CGATAAAGCGAGCAATGTTT	
actr2a-F	TTGATGGCGGGTTCTATGC	
actr2a-R	TCCTCGGATTCAGCGAGTG	
actr2b-F	TGCTATTTTACCACGACCCT	
actr2b-R	CACAACACCAGATAAACCTTGA	
bmp8a-F	TCGCTGGCTTCTCCATCCT	
bmp8a-R	ATCACATTCCCCGTCACAA	
actb1-F	CCGTGACATCAAGGAGAAGC	
actb1-R	TACCGCAAGATTCCATACCC	
EPC *actin*-F	TGTTCCAGCCATCCTTCTTG	qRT-PCR for EPC cells
EPC *actin*-R	TGATTTTCATTGTGCTGGGG	
EPC *ifn*-F	ATGAAAACTCAAATGTGGACGTA	
EPC *ifn*-R	GATAGTTTCCACCCATTTCCTTAA	
EPC *irf3*-F	AACAAGAATGACACTGCGGA	
EPC *irf3*-R	AACTCGGGAGGGACTTTCAT	
EPC *irf7*-F	AAAGTCTTCGTCAGCACCAGCG	
EPC *irf7*-R	CTCTCCGAAGCACAGGTAGATGGT	
EPC *tbk1*-F	TCAGAAGTTTGAGAACGGGAAGA	
EPC *tbk1*-R	CGTAGACCACGATGCGGTGTAAG	
EPC *mx*-F	GGCTGGAGCAGGTGTTGGTATC	
EPC *mx*-R	TCCACCAGGTCCGGCTTTGTTAA	
GCRV VP5-F	CTCCCCGTGAGCGTATTT	qRT-PCR for GCRV
GCRV VP5-R	GTTAGCAGCGGTAGTGACTTG	
P1 biotin probe-F	biotin-AGACCATTCCGGGAAAACCAA	EMSA
P1 biotin probe-R	biotin-TTGGTTTTCCCGGAATGGTCT	
P1 non-biotin probe-F	AGACCATTCCGGGAAAACCAA	
P1 non-biotin probe-R	TTGGTTTTCCCGGAATGGTCT	
P1 mutant non-biotin probe-F	AGACCAGCCCGGGGCAACCAA	
P1 mutant non-biotin probe-R	TTGGTTGCCCCGGGCTGGTCT	
P2 biotin probe-F	biotin-TTCAATTTACTAGAACTTCTC	
P2 biotin probe-R	Biotin-GAGAAGTTCTAGTAAATTGAA	
P2 non-biotin probe-F	TTCAATTTACTAGAACTTCTC	
P2 non-biotin probe-R	GAGAAGTTCTAGTAAATTGAA	
P2 mutant non-biotin probe-F	TTCAATGCACTAGGCCTTCTC	
P2 mutant non-biotin probe-R	GAGAAGGCCTAGTGCATTGAA	
bmp8a talen-F	TGGGCCTCGCTCTAAGC	TALEN
bmp8a talen-R	ACTGATCGAGACTTCTT	
bmp8a F1-F	GGAACTCTGAATCTGCGTCT	
bmp8a R1-R	TCACAGGAGGGCGAATAG	
bmp8a F2-F	GACAGACATTCAGGCACGTA	
bmp8a R2-R	GCCGTCCACTGCTATGAT	

847 Supplementary Table 1. Oligonucleotides used in this study.

848 **Supplementary Table 2**

Primer names	Sequences (5' to 3')	Applications
pcDNA3.1-bmp8a-F	CGGGATCCGCCACCATGGACAGACACGAGGT	Eukaryotic expression
pcDNA3.1-bmp8a-R	GGAATTCCTATAAACAGCCACAATTC	
pcDNA3.1-stat1a-F	GGGGTACCGCCACCATGACTCAGTGGTTGGAGC	
pcDNA3.1-stat1a-R	GCTCTAGACTATGTCATTGTCATCAAG	
pcDNA3.1-stat1b-F	GGGGTACCGCCACCATGACGCTCTGGAACCA	
pcDNA3.1-stat1b-R	GCTCTAGACTAAAACCTTGCAACGGGT	
pcDNA3.1-alk2-F	CCCAAGCTTGCCACCATGGGGCATTGCAGCAC	
pcDNA3.1-alk2-R	CGGGATCCTCAGCAGTCGGTTTTGCCCTT	
pcDNA3.1-alk3-F	CCCAAGCTTGCCACCATGCGTCAGCTTTTGT	
pcDNA3.1-alk3-R	CGGGATCCTCAGATTTTAATGTCTTGAGAT	
pcDNA3.1-alk6a-F	CGGGATCCGCCACCATGGATCTCTATAGGA	
pcDNA3.1-alk6a-R	GCTCTAGATCAGACTTTAATGTCCTGGGAT	
pcDNA3.1-actr2a-F	CCCAAGCTTGCCACCATGGGACCTGCAACAAA	
pcDNA3.1-actr2a-R	GGAATTCTCATAGACTAGACTCCTTTGGG	
pcDNA3.1-actr2b-F	CCCAAGCTTGCCACCATGTTCGCTTCTCTGCTC	
pcDNA3.1-actr2b-R	GGAATTCTCAGATGCTGGACTCTTTGGGC	
pcDNA3.1-bmpr2a-F	GGAATTCGCCACCATGGCAGTTGAAGGCCGAATA	
pcDNA3.1-bmpr2a-R	GCTCTAGATCAAAAGTCACAGTCATTAGGATCTG	
pcDNA3.1-bmpr2b-F	GGAATTCGCCACCATGAGAGTGCGGATCCTAAAC	
pcDNA3.1-bmpr2b-R	GCTCTAGATCACAGGCAGGTCATATCTGG	
pet-28a-stat1a-F	GGAATTCATGACTCAGTGGTTGGAGCTTC	Prokaryotic expression
pet-28a-stat1a-R	CCCAAGCTTTGTCATTGTCATCAAGTCTGC	
pet-28a-stat1b-F	CGGGATCCATGACGCTCTGGAACCAGCTG	
pet-28a-stat1b-R	CCGCTCGAGAAACCTTGCAACGGGTCTTG	
pGL3-bmp8a-promoter-F	GGGGTACCTCACTTTCGTCAATTGGTGAA	Luciferase assay
pGL3-bmp8a-promoter-R	CCGCTCGAGTGGTGTAGCGAAGAGCCCAGC	
pGL3-bmp8a-promoter-ΔP1-F	GGTCTGACTCCGTTTCAATTCTCTGTTAAGCTGATCTGACACAA	
pGL3-bmp8a-promoter-ΔP1-R	TTGAAACGGAGTCAGACCAGTTTTCAGAGTTGA	
pGL3-bmp8a-promoter-ΔP2-F	TAGTCAGACCACCAACGTCGGGTGAACAGCTAA	
pGL3-bmp8a-promoter-ΔP2-R	ACGTTGGTGGTCTGACTACCGTCTCGAAGTTCA	
pGL3-IFNφ1-promoter-F	TCTCGAGAAGTGAAGTGAAAGTGCA	
pGL3-IFNφ1-promoter-R	CAAGCTTGTTCTCATCTTTGCGTGT	
pGL3-IFNφ3-promoter-F	GGGTACCGTTCACTGAGCCTGCATG	
pGL3-IFNφ3-promoter-R	TCTCGAGGATGCCTATACGGAATCA	
pGL3-EPC IFN-promoter-F	GGGGTACCGACCTTGAAATACTTTGGAATCAGGT	
pGL3-EPC IFN-promoter-R	CCCAAGCTTGCACAAACATATACGTCCACATT	
pcmv-bmp8a-HA-F	AGCCCGGGCGGATCCAAGCTTGCCACCATGGACAGACACGA	CO-IP
pcmv-bmp8a-HA-R	ATCGAATTCCTGCAGAAGCTTTAAACAGCCACAATTCTTGACCA	
pcmv-alk6a-Flag-F	CGCTCTAGCCCGGGCGGATCCGCCACCATGGATCTCTATAGGAGC	
pcmv-alk6a-Flag-R	TTCCTGCAGAAGCTTGGATCCGACTTTAATGTCCTGGGATTCAGAC	
pcDNA3.1-alk6a-ΔGS-F	ATAGAGCAATCCCAGCTCCCTCTACTGGTGCAGCG	Dominant negative mutant
pcDNA3.1-alk6a-ΔGS-R	GAGCTGGGATTGCTCTATGAGATCCCGCAGAGA	
pcDNA3.1-irf3DN-F	GGGGTACCGCCACCATGGGATCTGAGGGCTCTCAA	
pcDNA3.1-irf3DN-R	GGAATTCTTAGCAGAGCTCCATCATTTG	
pcDNA3.1-irf7DN-F	GGGGTACCGCCACCATGAAGAGTGCGATCCAGAGTG	
pcDNA3.1-irf7DN-R	GGAATTCTTATTCCACTGAAGGCAGACC	
pcDNA3.1-stat1a-ΔC-F	TCCGAGCTCGGTACCAAGCTTATGACTCAGTGGTTGGAGCTTCA	
pcDNA3.1-stat1a-ΔC-R	CAGCGGTTTAAACTTAAGCTTTCAAATGATGTCAGGAAGTGAAACA	
pcDNA3.1-stat1b-ΔC-F	TCCGAGCTCGGTACCAAGCTTATGACGCTCTGGAACCAGCTG	
pcDNA3.1-stat1b-ΔC-R	CAGCGGTTTAAACTTAAGCTTTCACATGGAGATGGTTGCCAG	
pcDNA3.1-tbk1 K38M-F	CCGTCATGGTGTTCAACAACCTGGTGTTCAACAACCTGAGTTTCCTG	
pcDNA3.1-tbk1 K38M-R	TGTTGAACACCATGACGGCGTACAGATTGACGGCGTACAGATCGCC	

849 Supplementary Table 2. Oligonucleotides used in this study.

850